Canadian Journal of
Fisheries and
Aquatic Sciences

Article

Life-cycle modeling reveals high recovery potential of at-risk wild Chinook salmon via improved migrant survival

Gregory R. Jacobs[a,b,c], **Russell F. Thurow**[d], **Charles E. Petrosky**[e], **Craig W. Osenberg**[a,b], **and Seth J. Wenger**[a,b]

[a]Odum School of Ecology, University of Georgia, Athens, GA, USA; [b]River Basin Center, University of Georgia, Athens, GA, USA; [c]Department of Natural Resources and the Environment, Cornell University, Ithaca, NY, USA; [d]US Forest Service, Rocky Mountain Research Station (Emeritus), Salmon, ID, USA; [e]Idaho Department of Fish and Game (Retired), Boise, ID, USA

Corresponding author: **Gregory R. Jacobs** (email: gj93@cornell.edu)

Abstract

Chinook salmon (*Oncorhynchus tshawytscha*) in the Columbia River basin are threatened by anthropogenic changes to migratory corridors, estuaries, and natal habitats. Streams provide spatially heterogeneous natal habitats essential for salmon spawning and rearing life stages. We fit a statistical state-space model to salmon populations in Idaho's Middle Fork Salmon River (MFSR) to assess spatial variation in natal productivity and population growth. Our model integrated multiple long-term data sets to estimate variation in per-capita smolt production and smolt-to-adult (SAR) survival. Smolt production varied across stream segments, averaging 104.48 female smolts per spawning female, while SARs averaged 0.74%. Chinook salmon population growth rates exceeded replacement in 17% of segments (4 of 23). By increasing SARs to 1.8% (near the lower bound of Columbia River basin recovery targets), we predict that all 23 MFSR segments will yield positive population growth rates at contemporary (very low) spawner densities. Our analysis suggests that for Snake River basin populations within high-quality natal habitats, SAR improvements will elevate salmon population growth rates and enhance restoration of at-risk wild Chinook salmon.

Key words: dams, redds, restoration, migration, Bayesian statistics

Introduction

Salmon are ecologically, socially, and economically important fish and the focus of intensive and extensive management efforts across the northern hemisphere. After European settlement of North America, Pacific salmon stocks declined because of overharvest, habitat degradation, hatchery production, and the construction of hydropower dams that blocked or degraded migratory corridors (NMFS 2000). Pacific salmon declines prompted intense conservation and restoration efforts and, in several cases, listing under the US Endangered Species Act (ESA; Nehlsen et al. 1991; NMFS 1992). Despite such efforts, many Chinook salmon (*Oncorhynchus tshawytscha*) stocks have been unable to overcome the deleterious effects of migration barriers, habitat alterations, and climate change (Budy et al. 2002; Crozier et al. 2019, 2020; Faulkner et al. 2019; Petrosky et al. 2020), remain far below historical abundances, and face extinction (Johnson et al. 2021; Williams et al. 2021).

To persist, salmon must have sufficient reproduction and juvenile survival in freshwater (natal) habitat and sufficiently high survival from the out-migrating smolt stage to the returning adult spawner stage. The latter, measured as the smolt-to-adult return rate (SAR), is determined by smolt mortality while migrating to the ocean, sub-adult mortality in the ocean, and adult mortality on the return migration (Petrosky and Schaller 2010; Haeseker et al. 2012; Schaller et al. 2014; Petrosky et al. 2020). Survival is affected by dams and obstructions (Schaller et al. 2014), biotic interactions (e.g., predation by pinnipeds and orcas; Chasco et al. 2017*a*, 2017*b*), and climate-driven changes in ocean and migratory corridor conditions (Crozier et al. 2019, 2020).

Persistence also depends on the quality of natal habitat, which is likely to exhibit high spatial variability resulting from the biophysical heterogeneity of stream environments (Fausch et al. 2002) and strong natal homing behavior (Quinn 2018). High spatial heterogeneity in natal productivity combined with low SARs could lead to the maintenance of regional stocks by only a few exceptionally productive "core" stream segments (Isaak and Thurow 2006). Disturbances at these core sites could lead to regional extirpation. Understanding the spatial heterogeneity of natal habitat is therefore crucial for effectively targeting management actions (NMFS 1992, 2017; ICTRT 2003).

Inference on spatial variation in population dynamics is often limited by a lack of fine-scale census data, even for well-studied taxa such as salmonids. Smolt production

rates of Chinook salmon, for example, have often been estimated at relatively coarse spatial scales (Petrosky et al. 2001; Wilson 2003). However, inference on the dynamics of Chinook salmon from analysis of spawner distributions at finer spatial scales has proven informative in systems like the Middle Fork Salmon River (MFSR), where high-resolution spatial data are available (Isaak and Thurow 2006; Isaak et al. 2007; Thurow et al. 2020; Jacobs et al. 2021). These high-resolution data provide evidence of the spatial scale of habitat use and dispersal (Isaak and Thurow 2006; Hamann and Kennedy 2012) and population genetic structure (Neville et al. 2006). The MFSR hosts hundreds of kilometers of highly connected, high-quality natal salmon habitat in a landscape predominantly protected as federally designated wilderness (Thurow et al. 2020). This basin is notable for its wild and diverse Chinook salmon stocks (Neville et al. 2006; Thurow et al. 2020) and functioning natural landscape processes (e.g., fire regime, hydrogeological processes, and patch connectivity; Jacobs et al. 2021) that have been minimally altered by humans. Population genetic structure at spatial scales similar to the distinct stream segments identified by Isaak and Thurow (2006) and Neville et al. (2006) suggests that population dynamics may reasonably be assumed isolated at this segment scale. Thus, the MFSR basin is well suited for investigating spatial variation in salmon population dynamics in intact natal habitat (Schaller et al. 1999, 2014; Thurow 2000; Isaak and Thurow 2006; Copeland et al. 2014; Thurow et al. 2020).

Here we focus on wild spring/summer run, stream-type Chinook salmon, hereafter referred to as "Chinook salmon", that spawn in the MFSR (Healey 1991; Matthews and Waples 1991; Thurow et al. 2020). These fish belong to the Snake River spring/summer Chinook salmon Evolutionarily Significant Unit (ESU), currently listed as "Threatened" under ESA (NMFS 1992). Chinook salmon in this ESU had an estimated mean SAR of 0.76% from 1994 to 2019 (McCann et al. 2020), which is far below the Northwest Power and Conservation Council's (NPCC) target SAR of 2%–6% deemed necessary to recover the stock (NPCC 2003). Although benefits to Chinook salmon population growth have been achieved by increasing the productivity of natal habitat (Louhi et al. 2016; Copeland et al. 2021), the potential for recovery via tributary restoration alone is low in the Snake River ESU, where high-quality natal streams are abundant (Budy and Schaller 2007) and outside-basin conditions strongly influence SARs (Petrosky et al. 2020; Storch et al. 2022). While management options for affecting marine conditions are limited (ISAB 2018), recent analyses suggest that improvements to the lower Snake River migration corridor, and specifically the breach or removal of Snake River dams (NOAA 2022; AFS 2023), may increase in-river and ocean survival sufficiently to meet SAR targets set by the NPCC (McCann et al. 2017; Storch et al. 2022).

Here we build on decades of prior research to construct a statistical life-cycle model for Chinook salmon subpopulations in the MFSR, estimated using a Bayesian state-space model framework and informed by multiple long-term data sets. We used this model to estimate per-capita reproductive rates of Chinook salmon within the MFSR, the spatiotemporal variation in these rates, and the sensitivity of basin-wide population growth conditions to outside-basin mortality. Our goals were to (1) estimate the spatial distribution of productive stream segments for Chinook salmon in the MFSR, and (2) predict variation in the number of MFSR segments capable of supporting Chinook salmon population growth in response to increases in SARs.

Materials and methods

Site description

The 7,330 km^2 MFSR basin in central Idaho, USA, supports an estimated 777 km of contiguous, intact Chinook salmon spawning streams flowing through a mountainous landscape largely unaltered by humans, with a majority protected within the Frank Church River of No Return Wilderness (Thurow et al. 2020; Fig. 1). The MFSR enters the Salmon River, a major tributary to the Snake River, which in turn feeds the larger Columbia River in the Pacific Northwest of North America. The migratory corridor for these fish, linking the MFSR and the Pacific Ocean, has been altered by eight large dams operating in the Columbia River System that impound 520 km of formerly free-flowing reaches of the Columbia and Snake Rivers (hereafter, the "hydrosystem"; Petrosky and Schaller 2010). Downstream of the hydrosystem, the migratory corridor extends through the Lower Columbia River and Estuary (LCRE) before entering the Pacific Ocean. Counts of spawning Chinook salmon nests (hereafter "redds") have been monitored annually in a subset of index reaches in the MFSR since 1957 (Thurow et al. 2020). We focus our analysis on annual, spatially continuous, georeferenced redd surveys that have been conducted since 1995 (Thurow 2000), which we organized into annual redd counts in each of the 23 distinct river segments identified by Isaak and Thurow (2006).

Life-cycle model

Snake River Chinook salmon spawn from July to September, when females excavate redds in gravel substrates, spawn, and bury fertilized eggs. Female Chinook salmon defend redds from predators and conspecific redd-building competitors until death. Eggs incubate over winter, hatch the next spring as larvae, and emerge as fry. Fry grow into parr that remain in freshwater habitats until migration. Most MFSR Chinook salmon begin their migration to the ocean at age 1 (i.e., during their second spring), though parr may spend from <1 year to 2 years in freshwater prior to out-migration and transformation from parr to smolts (Copeland and Venditti 2009). Flow conditions, hydrosystem operations (e.g., spill, surface passage), and departure date influence out-migration from the MFSR to the ocean, which may take between 10 days and 1.5 months (McCann et al. 2020). Travel times were much faster before the dams (Petrosky and Schaller 2010). Mature adults returning from the ocean arrive at Bonneville Dam (the lowermost dam), navigate eight hydroelectric dams (Lower Granite Dam is the uppermost and eighth dam), and return to spawn in the MFSR. Most female Chinook salmon in the MFSR, the object of our population model, spend 2–4 years in the ocean, returning to spawn at age 4, 5, or 6 (Poole

Fig. 1. The Middle Fork Salmon River basin, Idaho USA (black outline), its stream segments (colored stream lines labeled with letters of the alphabet), and ICTRT-defined (2003) "Population" sub-basins: Bear Valley Creek (BEA), Big Creek (BIG), Camas Creek (CAM), the lower MFSR mainstem (LMA), Loon Creek (LOO), Marsh Creek (MAR), Sulphur Creek (SUL), and the upper MFSR mainstem (UMA). The inset map depicts the Columbia River basin outlined in black, the Columbia River and major tributaries in blue, and the MFSR watershed in red. This map was created using Esri ArcMap 10.8 using the ArcGIS Online World Topographic Map basemap (Esri n.d.); projection is NAD 1983 Albers Equal-Area Conic.

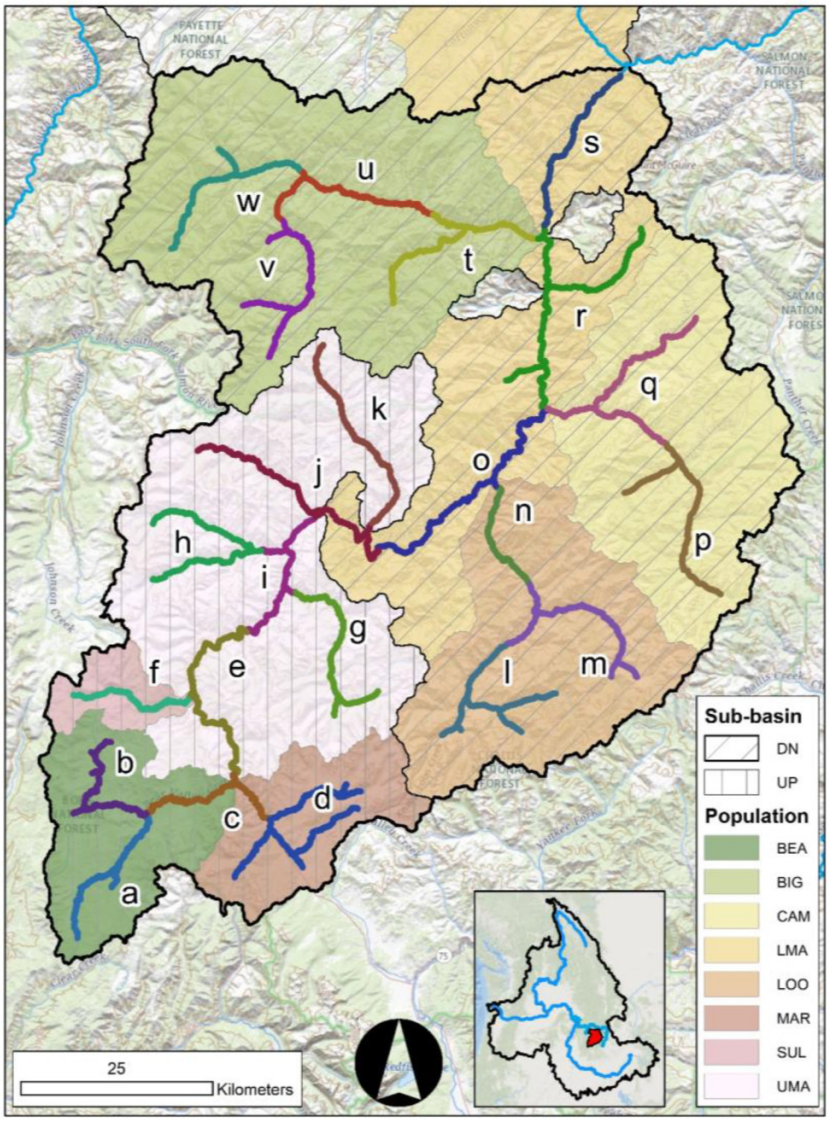

et al. 2022). Since Chinook salmon are semelparous, no reproductive adults survive to contribute to the next year's abundance.

We defined a Chinook salmon life cycle consisting of five age classes and one multi-age spawning class, which comprise the state variables (Fig. 2): N_1 (age 1 female smolts), N_1–N_5 (age 2–5 marine phase females), and S (the total number of mature age 4–6 females, R_4–R_6, that build redds; i.e., $S = R_4 + R_5 + R_6$). Parameters governing changes in state variables over time included survival probabilities, stage transition probabilities, and reproductive rates (Table S1). We modeled the dynamics of Chinook salmon females on a 1-year time step (t) and across MFSR river segments (i), treating segments as isolated populations closed to immigration and emigration. Since MFSR Chinook salmon are at historically low density in the MFSR (1%–3% of 1960s abundances; Thurow et al. 2020), we fit a model that does not structurally estimate density-dependent population growth but implicitly accounts for it by estimating process heterogeneity in space and time. Our model is thus built around a simple geometric population growth function: $R = Sb\phi$, where recruitment of reproductive adults (R) equals the per-capita production of smolts (b) by spawning adults (S) multiplied by survival-to-maturity (ϕ). We define per-capita smolt production, the product of egg production, hatching success, and survival of parr, as the number of migrating smolts that survive to the first (upstream-most) dam in the migration corridor. In our model, we allow per-capita smolt production to vary spa-

Fig. 2. Chinook salmon life cycle used to structure our integrated Bayesian state-space population model. Large arrows represent smolt-to-adult return probability (SAR) and smolt production rate (b), and small arrows represent survival and maturation processes that comprise SAR. The S stage represents spawning adults composed of multiple ages, and the N stages represent smolts (N_1) and pre-migratory ocean residents (N_2–N_5). Subscripts on stages indicate the age of the fish in those stages. Green indicates freshwater stages and transitions; blue indicates marine or migratory stages and transitions.

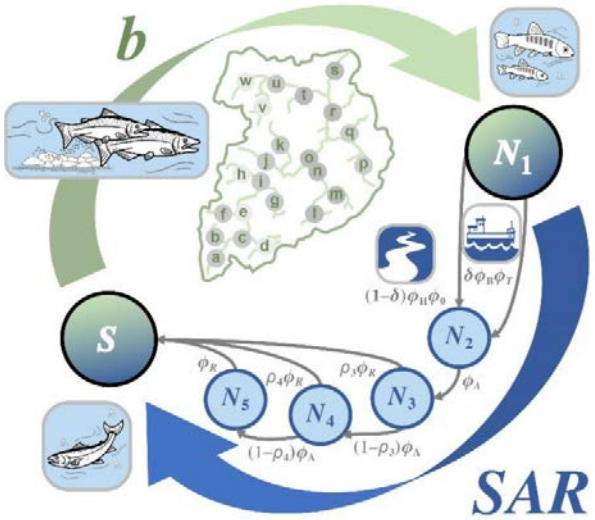

tially within the MFSR and temporally across years. Survival-to-maturity in our model is equivalent to SAR, incorporating juvenile survival during the out-migration year (through the hydrosystem and during their initial ocean residence period), sub-adult ocean survival, and adult survival during return migration upstream through the hydrosystem (at age 4, 5, or 6).

We estimated the production of smolts at stream segment i and time $t+2$ as the product of a spatially and temporally heterogeneous smolt production rate, $b_{(i,t)}$, and the number of reproductive females in that stream segment at time t:

$$(1) \qquad N_{1(i,t+2)} = S_{(i,t)} b_{(i,t)}$$

Salmon smolts from the MFSR migrate through the hydrosystem by one of two pathways: (1) via trapping and transport by barge along the migratory corridor; and (2) via "in-river" passage through (or over) eight dams, associated reservoirs, and intervening river corridors under their own power. The survival of transported (or T-group) and in-river (or H-group) fish during the migration year is further subdivided into "hydrosystem" survival and "early ocean" survival. Hydrosystem survival is either a function of capture and barging conditions for transported fish, $\phi_B = 0.98$ (McMichael et al. 2011), or a function of hydrosystem conditions during the migration year (t) for in-river fish, $\phi_{H(t)}$. Smolts that survive passage downstream through the hydrosystem must next survive conditions in the Columbia River estuary and nearshore Pacific Ocean through their first winter at sea (hereafter "early ocean survival"), which we denote as $\phi_{O(t)}$ for in-river fish and $\phi_{T(t)}$ for transported fish. The survival of individuals through these two pathways combines to determine population-level survival during the migration year according to the proportion of fish that experience the "transport" pathway, $\delta_{(t)}$, in contrast to the "in-river" pathway,

$$(2) \qquad N_{2(i,t+1)} = N_{1(i,t)} \left(\left(1 - \delta_{(t)}\right) \phi_{H(t)} \phi_{O(t)} + \delta_{(t)} \phi_B \phi_{T(t)} \right)$$

After the first winter at sea, we model the ocean survival of salmon as a function of an assumed annual ocean survival rate, $\phi_A = 0.80$ (approximated from Ricker 1976), and maturation probabilities that control whether age-3 or age-4 fish return to spawn the following year ($\rho_{3(t)}$, $\rho_{4(t)}$). We assumed all age-3 females remain in the ocean, a portion of age-4 and age-5 females return as spawners ($\rho_{3(t)}$ and $\rho_{4(t)}$, respectively), and all age-6 females return as spawners. Age-specific abundances, annual ocean survival, and maturation probabilities then define the distribution of ages among ocean residents,

$$(3) \qquad \begin{aligned} N_{3(i,t+1)} &= N_{2(i,t)} \phi_A \\ N_{4(i,t+1)} &= N_{3(i,t)} \phi_A \left(1 - \rho_{3(t)}\right) \\ N_{5(i,t+1)} &= N_{4(i,t)} \phi_A \left(1 - \rho_{4(t)}\right) \end{aligned}$$

Similarly, these parameters define the distribution of ages among the breeding stock, but with an additional "return" survival term, ϕ_R, to account for mortality as adults migrate upstream through the hydrosystem,

$$(4) \qquad \begin{aligned} R_{4(i,t+1)} &= N_{3(i,t)} \phi_A \rho_{3(t)} \phi_R \\ R_{5(i,t+1)} &= N_{4(i,t)} \phi_A \rho_{4(t)} \phi_R \\ R_{6(i,t+1)} &= N_{5(i,t)} \phi_A \phi_R \end{aligned}$$

We assume that all adult fish that survive passage upstream through the hydrosystem successfully spawn in their natal habitat. Thus, the number of redds in each segment of the MFSR is the number of returning adult females summed across all ages:

$$(5) \qquad S_{(i,t)} = R_{4(i,t)} + R_{5(i,t)} + R_{6(i,t)}$$

Data and model fitting

Redd counts

Annual Chinook salmon redd surveys were conducted at the end of the spawning season in September from 1995 through 2018 via low-altitude helicopter flights supplemented by ground-based surveys using methods described by Thurow (2000). Surveys employed a spatially continuous sampling design (Fausch et al. 2002), and individual redd locations were georeferenced with a global positioning system. Streams deemed too small or steep to be accessible to Chinook salmon were omitted from the survey area (Thurow 2000; Isaak and Thurow 2006). Georeferenced redd locations were snapped to the stream network and aggregated at the scale of discrete river segments identified by Isaak

and Thurow (2006). The average segment length was 33.8 km (range = 17–54). Aggregated redd count data comprised a data matrix of counts across 23 segments (*i*) for 24 years (*t*). We modeled the number of redds observed using an over-dispersed Poisson likelihood function (eq. S18).

Carcass fin age

From 1998 to 2019, Idaho Department of Fish and Game (IDFG) monitored the age and sex of adult Chinook salmon in the MFSR via post-spawning carcass surveys (M. Davison, IDFG, personal communication).We used age estimates of females derived from counts of annual growth rings in fin ray cross-sections to define our spawner age dataset. Three age classes were observed among female Chinook salmon in the MFSR during this time period: age 4, 5, and 6. We modeled segment-scale redd counts as a function of spawner age distributions at coarser-scale "populations" ($n = 8$ in our study area) defined by the Interior Columbia Technical Recovery Team (ICTRT 2003; Fig. 1) because the distribution of carcass survey points was too sparse at the segment scale. We modeled the number of female carcasses observed at each age in each year as a function of the proportion of returning females at the age predicted by our model (eq. S17).

Hydrosystem passage

We used count data for PIT-tagged Snake River wild aggregate spring/summer Chinook salmon (excluding jacks) from the Comparative Survival Study (CSS) for the 1994–2019 migratory cohorts (McCann et al. 2020). We distinguished "in-river" fish that avoided bypass or transport at designated Snake River collector dams (Lower Granite, Little Goose, Lower Monumental) from "transported" fish that were captured and transported from one of the collector dams to below Bonneville Dam, according to the definitions of the C_0 and T_0 passage groups in McCann et al. (2020). We estimated the cohort-specific survival and observation probability of Chinook salmon by tracking observations across three different migratory phases: river transit as smolts, ocean residency, and river transit as returning adults. From these phases, we defined four release and recapture (or re-observation) occasions: (1) passage at Lower Granite Dam as smolts (LGR), (2) observation at Bonneville Dam as smolts (BON), (3) observation at Bonneville Dam as adults (BOA), and (4) observation at Lower Granite Dam as adults (LGA). Counts at LGR during the smolt stage were estimated quantities for the C_0 and T_0 groups defined in McCann et al. (2020), rounded to the nearest integer, whereas the PIT tag counts at BON, BOA, and LGA were from data used in the CSS (McCann et al. 2020). Counts at LGR, BON, BOA, and LGA were taken from the CSS (McCann et al. 2020) or provided upon request when not presented in CSS reports (J. McCann (personal communication)). These hydrosystem PIT tag passage counts were formatted as multinomial capture histories for capture-mark–recapture analysis (Kéry and Schaub 2012; Supplementary material). We modeled mark–recapture count data using a multinomial likelihood function for each of the in-river (eq. S15) and transported (eq. S16) smolt groups. We also specified, as data, point estimates of in-river hydrosystem survival for in-river smolts and transport probability for transported smolts of Snake River wild aggregate spring/summer Chinook salmon presented by McCann et al. (2020) for the 25-year period from 1994 to 2018. These time series data were drawn from model-estimated in-river hydrosystem smolt survival and smolt transport probability using a Beta likelihood function for each (eq. S14).

Survival covariates

We allowed in-river and early ocean survival to vary according to six migration year covariates found to drive variation in Chinook salmon survival and hydrosystem passage (Schaller et al. 2014; McCann et al. 2020): (1) SST, May–June–July Sea Surface Temperature from the Comprehensive Ocean-Atmosphere Data Set summarizing observations from buoys and ships near the mouth of the Columbia River (Slutz et al. 1985; McCann et al. 2021); (2) UWI, Bakun Upwelling Index for 45 N latitude, 125 W longitude during April (https://www.cpc.ncep.noaa.gov/products/GODAS/coastal_upwelling.shtml; Accessed: 3 November 2020); (3) PDO, average May-June-July Pacific Decadal Oscillation index (http://research.jisao.Washington.edu/pdo/PDO.latest.txt; accessed 6 October 2020); (4) WTT, Water Transit Time through the Columbia River hydrosystem from Lower Granite Dam to Bonneville Dam (McCann et al. 2021); (5) PH, the average number of dam power house passages (as opposed to comparatively less dangerous passages via spill) predicted for outmigrating Snake River Chinook salmon (PITPH, McCann et al. 2021); and (6) Z, a binary variable for smolt transport barge schedule, which differed between 1993–2006 and 2007–2017 (Widener et al. 2021). In our covariate data set, SST averaged 13.698 °C (SD 0.835) from 1988 to 2018, UWI averaged −2.355 (SD 19.216) from 1988 to 2019, PDO averaged −0.188 (SD 1.1090) from 1988 to 2019, PH averaged 2.696 powerhouse passages (SD 0.912) from 1994 to 2019, and WTT averaged 19.106 days (SD 5.436) from 1988 to 2019, and *Z* was equal to 0 for 1993–2006 and 1 for all years after 2006 (Fig. S1).

Model fitting and assessment

We defined six response variables in our integrated model: (1) redd counts, (2) spawner ages, (3) hydrosystem passage counts for in-river group fish, (4) hydrosystem passage counts for transported group fish, (5) smolt survival probabilities for in-river fish, and (6) smolt transport probabilities. Redd count data varied by segment and year; spawner age data are counts of female carcasses that varied by ICTRT population, year, and age; hydrosystem passage datasets varied by migration year cohort and passage facility; and smolt survival and smolt transport datasets varied by year. The joint distribution equation for our model (eq. S25), parameter definitions (Table S1), and parameter estimation details are in the supplementary material file.

We fit our model using MCMC sampling in JAGS 4.3.0 (Plummer 2017) with the R package "runjags" (Denwood 2016) in R version 4.2.1 (R Core Team 2022). We ran our model for a 1,000-iteration adaptation period and 1,000,000 iterations of burn-in, followed by 500,000 iterations of posterior sampling thinned to every 20 iterations across 5 chains. We considered the model to have converged if the convergence diagnostic, $\widehat{R}$ (Gelman and Rubin 1992), was below 1.1 for all estimated parameters. We also assessed convergence by visually inspecting and comparing each chain's MCMC sample traces and posterior sampling distributions. We evaluated goodness of fit by plotting the Freeman–Tukey discrepancy statistic for real data versus that from simulated data and calculated a Bayesian *P*-value indicating the probability that the simulated discrepancy would be more extreme than that of our empirical data (Gelman 2013; Conn et al. 2018).

Simulation analysis

The number of spawning adult females produced per parental redd ($\lambda_{(i,t)}$) for each segment i and brood year t was estimated as the product of smolt production during the brood year ($b_{(i,t)}$) and SARs for subsequent smolt migration-year cohorts ($\phi_{\mathrm{SAR}(t)}$):

$$\lambda_{i,t} = b_{(i,t)}\phi_{\mathrm{SAR}(t+2)} \quad (6)$$

We conducted our simulation analysis using brood years 1988 through 2016, the last year with a corresponding $\phi_{\mathrm{SAR}(t)}$ estimate in our model.

To assess the effect of SAR on population growth associated with each segment, we estimated $\lambda_{(i,t)}$ for each segment (i) in each cohort year (t) by varying average ϕ_{SAR} from 1% to 2% by increments of 0.2% and from 3% to 6% by increments of 1%, covering the range of established SAR goals for Chinook salmon recovery (2%–6%; NPCC 2003). All simulations were conducted by subsampling 999 iterations from model posteriors in each of our five parallel chains ($n = 4995$ subsampled posterior iterations) to simulate the distribution of λ under ϕ_{SAR} scenarios during our study period. To propagate uncertainty in birth and survival parameter estimates, we first calculated the empirical geometric mean of $\phi_{\mathrm{SAR}(t)}$ ($\overline{\phi_{\mathrm{SAR}}}$) from the migration years 1990–2018 (brood years 1988–2016) for each posterior sampling iteration subsampled from our model. We then calculated a ϕ_{SAR} correction factor for each simulation scenario ($x_{(\mathrm{sim})}$) by dividing that scenario's target ϕ_{SAR} ($\mathrm{SAR}_{(\mathrm{sim})}$) by the median of $\overline{\phi_{\mathrm{SAR}}}$: $x_{(\mathrm{sim})} = \mathrm{SAR}_{(\mathrm{sim})}/\mathrm{median}\left(\overline{\phi_{\mathrm{SAR}}}\right)$. We multiplied the distribution of $\overline{\phi_{\mathrm{SAR}}}$ subsampled from our model posteriors by each scenario's $x_{(\mathrm{sim})}$, resulting in a distribution of simulated $\overline{\phi_{\mathrm{SAR}}}$ for each scenario with a median exactly equal to the target $\mathrm{SAR}_{(\mathrm{sim})}$ and variance proportional to the variance of the uncorrected $\overline{\phi_{\mathrm{SAR}}}$ samples. For each scenario, we calculated the posterior mean, median, and modal number of segments with $\lambda > 1$ (indicating positive population growth). We also compared these simulations against our baseline using the estimated SAR.

Results

Data summary

Redd counts

Our redd count dataset included 18,468 redds observed across 777 km of MFSR streams from 1995 to 2018. The smallest basin-wide count occurred in 1995 (20 redds), and the largest count was in 2,003 (2,271 redds), with an average annual MFSR-wide redd count total of 770 (SD 593) and an oscillating trend through the survey period (Supplementary material, Fig. S2). In some years, a small number of segments were not surveyed because of turbid conditions or poor flight conditions during storms. Redd counts in the unsurveyed segments ("s" in 1995–1999, "r" in 1995, "q" in 1995, and "m" and "n" in 2013) were estimated as stochastic variables in our model, which allowed their imputation with associated uncertainty.

Carcass age

From 1998 to 2019, 2,316 female carcass age estimates were composed of three age classes: 1,190 were age 4, 1,099 were age 5, and 27 were age 6. Most female ages were estimated from carcasses collected in upper MFSR sub-basin populations (1853), and 463 age estimates were from carcasses in lower sub-basin populations (Fig. 1 and Table S2).

Hydrosystem passage

Chinook salmon smolts were diverted from in-river passage and transported by barge with an average CSS-estimated probability of 0.56 (SD 0.27) from 1994 to 2019, 0.79 (SD 0.12) from 1994 to 2006, and 0.32 (SD 0.13) from 2007 to 2019 (McCann et al. 2020). We assumed the transport survival probability was 0.98 (McMichael et al. 2011). Chinook salmon smolts that remained in-river survived migration from Lower Granite Dam to Bonneville Dam with an average CSS-estimated probability of 0.53 (SD 0.13; range: 0.20–0.68).

Model results

All parameters had a $\widehat{R}$ score below 1.1, consistent with model convergence, and posterior sampling chains appeared adequately mixed. Bayesian P-values based on the Freeman–Tukey discrepancy statistic were $P_{T(y_{\mathrm{redd}})} = 0.15$ for redd counts, and $P_{\mathrm{H}(m_{\mathrm{H}})} = 0.14$ and $P_{\mathrm{T}(m_{\mathrm{t}})} = 0.13$ for multinomial capture–mark–recapture datasets (Fig. S3). Visual assessment of simulated vs. observed SARs (Fig. S2), redd counts (Fig. S4), and redd count quantiles (Fig. S5) suggested our model was moderately well-specified.

Reproduction

The posterior median of our MFSR-wide mean smolt production rate was 104.48 smolts per female with a 90% Highest Density Interval (HDI) of 67.6–161.1. Fitted random variance terms suggested that the standard deviation (SD) of smolt pro-

Fig. 3. Spatial distribution of reproductive rate, *b* (female smolts per redd) and population growth, λ (redds per redd). In dot-whisker plots (*a, b*), dots indicate the median of posterior samples, thick lines the 90% highest density interval, and thin lines the 95% highest density interval. Panel (*a*) shows the reproductive rate (*b*) for each spatial unit (i.e., segment). Panel (*b*) shows the growth rate (λ) for each spatial unit. Panel (*c*) depicts the approximate spatial distribution of median growth rate estimates across the MFSR (blue line) and its watershed (black outline), where points are labeled by segment to match median and credible interval plots. Colors range from dark to light with increasing λ.

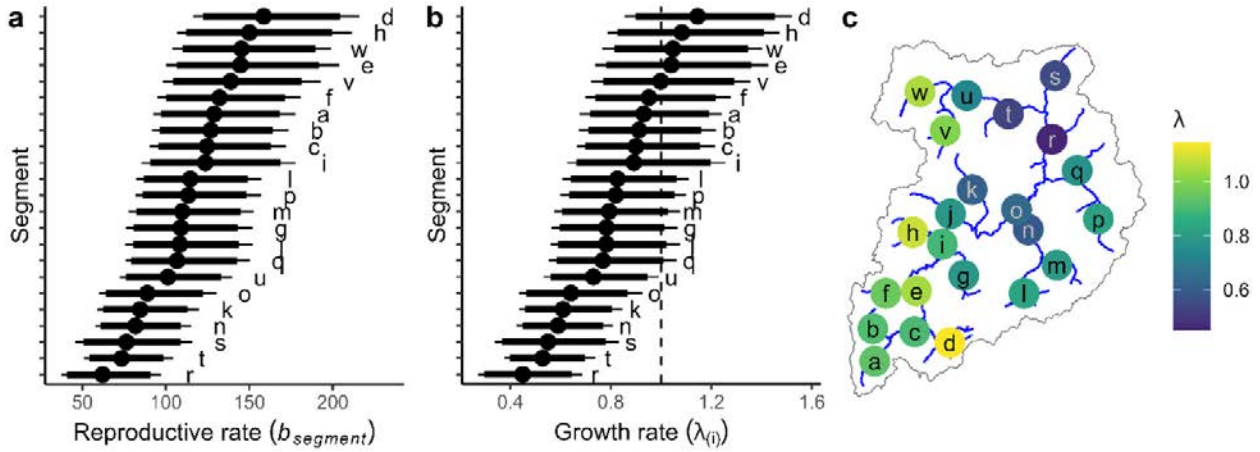

duction among years, 1.69 (HDI 1.26–2.15), was substantially larger than the SD among segments, 0.27 (HDI 0.18–0.38), and the SD of random segment × year variation, 0.32 (HDI 0.23–0.42). Segment-specific estimates of smolt production (female smolts per redd, *b*) ranged from 62.8 (90% HDI 37.4–87.4) for segment "r" to 159.5 (90% HDI 116.9–201.6) for segment "d" (see Fig. 1).

Transport, out-migration, and survival

The average proportion of wild Chinook salmon smolts transported, $\delta_{(t)}$, was 0.78 prior to 2007 and 0.33 during and after 2007, varying interannually with a logit-scale SD of 0.37 (Table S3). Our estimate of survival for salmon out-migrating through the hydrosystem ($\phi_{H(t)}$) was most strongly associated with PH and a random year effect, with a weak effect from WTT (Table S3). Early ocean survival for in-river fish ($\phi_{O(t)}$) covaried most strongly with SST, UWI, and WTT, with weak effects of PDO and PH (Table S3). Early ocean survival coefficients were similar for fish transported by barge ($\phi_{T(t)}$) (Table S3). Resulting early ocean survival estimates varied among years between 0.004 and 0.08 for in-river fish and between 0.002 and 0.06 for transported fish. Survival for returning adult salmon traversing the Columbia River hydrosystem from Bonneville Dam to Lower Granite Dam (ϕ_R) was 0.87 (90% HDI 0.800–0.938).

Maturation.

The probability of maturing at age 4 increased across our study period from lows of near 0.25 in the mid-1990s to highs near 0.75 approaching 2020, but with a high SD between sequential years of 0.89 on the logit scale (Fig. S6). The estimated probability of an age-4 fish maturing at age 5 (ρ_4) was 0.97 (HDI 0.96–0.98).

SAR and population growth

The SAR for the in-river smolt passage group, $SAR_{H(t)}$ (specific to the migration year cohort, *t*), varied annually between 0.1% and 3.0%, with an among-year arithmetic mean of 0.87% and a geometric mean of 0.62% (Fig. S1*a*). The SAR for the transported group, $SAR_{T(t)}$, varied between 0.1% and 2.6%, with an among-year arithmetic mean of 0.97% and a geometric mean of 0.76% (Fig. S1*b*). The among-year geometric mean of overall SAR, ϕ_{SAR}, had a posterior median of 0.74% (90% HDI 0.64–0.84) between 1988 and 2019, ranging from its lowest value of 0.1% in 1993 to its highest value of 2.7% in 1999. The basin-wide average smolt production rate and geometric mean SAR combined to yield an average population growth rate of λ=0.77, or a decline of 23% per generation. Population growth rate estimates for individual segments deviated from this average according to the segment random effect on smolt production in eq. S1 (Supplementary material) and ranged from 0.45 (90% HDI 0.28–0.63) for segment "r" to 1.15 (90% HDI 0.87–1.42) for segment "d". Geometric mean growth rates, λ, were >1 for 4 of 23 segments, although the HDI for these five segments all contained λ=1 (Fig. 3). The remaining 18 segments had λ<1, including one segment where λ=0.9982 and eight segments with credible intervals that did not include 1 (Fig. 3).

Simulation analysis

The posterior probability that all 23 segments in the MFSR supported positive Chinook salmon population growth (i.e., λ>1) was essentially zero. In the simulation analysis, 0 out of 4,995 posterior sampling iterations had λ>1 in all segments. Despite high variability in population growth rates at low SAR, elevating ϕ_{SAR} increased the number of productive segments and decreased its spread (Figs. 4*a*–4*f*). A simulated increase in SAR from 0.74% (contemporary conditions) to 1%

Fig. 4. Predicted number and location of MFSR river segments with positive Chinook salmon population growth rates under Snake River smolt-to-adult return (SAR) survival scenarios. Horizontal bar plots indicate posterior distributions of the number of MFSR river segments (23 total) with growth rates above replacement ($\lambda>1$) and black dots indicate the median. Map panels next to bar plots indicate the locations of the segments most likely to have growth rates above replacement under each SAR scenario, with colors ranging from dark to light with increasing λ.

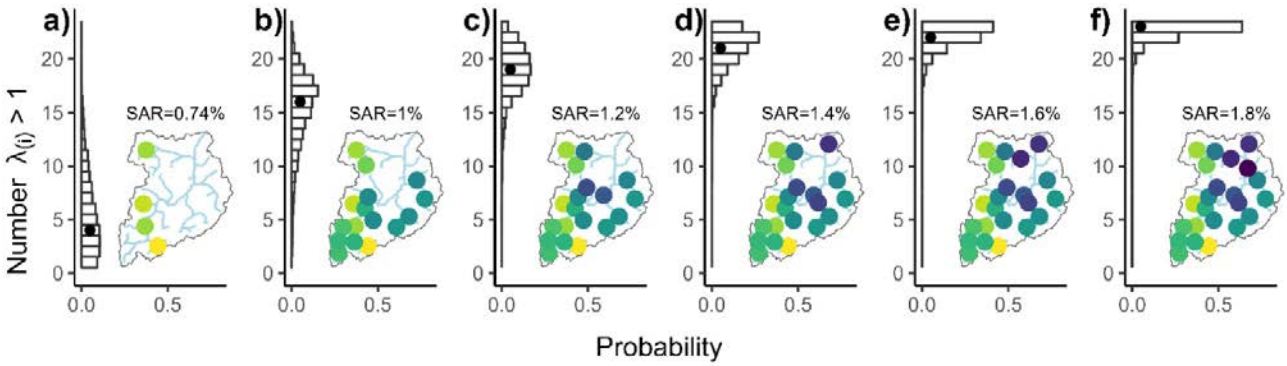

increased the number of productive segments from 5/23 to 16/23 (Fig. 4*a*). All 23 MFSR segments were predicted to support positive population growth for Chinook salmon at 1.8% SAR or higher (Figs. 4 and 5).

Discussion

Chinook salmon are in decline in the MFSR. Despite an abundance of high-quality natal habitat, our results suggest that a hypothetically "average" stream segment in the MFSR cannot produce enough smolts to overcome mortality that occurs outside of the basin. We estimate that since 1995, Chinook salmon have declined in 83% of stream segments that comprise the MFSR (i.e., $\lambda<1$ in 19/23 segments), supporting the conclusion that a minority of "core" stream segments are responsible for the continued persistence of Chinook salmon in the basin (Isaak and Thurow 2006). This narrow portfolio of viable spawning and rearing habitats (those with $\lambda>1$) is threatened by persistent anthropogenic stressors such as climate change, which will continue to erode both inland stream habitats and ocean conditions (Crozier et al. 2021; Jacobs et al. 2021). We conclude that the low proportion of sub-populations with positive growth, high interannual variation in demographic rates, and low abundances that we observed represent a high extirpation risk for Chinook salmon in the MFSR, which corroborates recent status assessments (e.g., Thurow et al. 2020; Johnson et al. 2021; Ford 2022).

Sub-populations of salmon are distributed across distinct natal habitats within and among river networks. In the MFSR, persistent, spatially distinct spawning aggregations (Isaak and Thurow 2006) and fine-scale population genetic structure (Neville et al. 2006) support our delineation of spatial sub-populations at a finer scale than those defined by the ICTRT (2003). In combination with low levels of connectivity, spatial heterogeneity can confer stability across metapopulations when sub-population fluctuations are asynchronous: local re-colonization (or immigration into low-density populations) from a regional metapopulation pool reduces the risk of synchronous extinctions (Heino et al. 1997; Sutcliffe et al. 1997). However, we found that synchronous temporal heterogeneity in smolt production rate ($\sigma_{b(year)} = 1.69$) was much larger than its spatial heterogeneity ($\sigma_{b(seg)} = 0.27$), suggesting relatively high synchrony among MFSR sub-populations, as also reported by Isaak et al. (2003). Under current conditions, high temporal synchrony likely impedes the potential resilience of Chinook salmon in this system (Isaak et al. 2007). Under high temporal synchrony, sub-population booms and busts will rarely be out-of-phase, a phenomenon that would slow the "rescue" of low-abundance reaches in the MFSR by more productive "core" habitats. Furthermore, analysis of the wild MFSR Chinook salmon population genetic structure (Neville et al. 2006) suggests that this synchrony is not a result of high dispersal among stream segments.

Spatial heterogeneity may be expected to increase with spatial scale as more widely separated pairs of sub-populations become increasingly isolated from one another. Thorson et al. (2014) reported that spatial variation of Chinook salmon parr productivity (among-population SD = 1.11) was much larger than its synchronous variation in time (among-year SD = 0.67) across 15 populations in the Salmon River spread over a larger spatial domain than segments in our study. Although hatcheries influenced the dynamics of nine of the 15 populations in Thorson et al. (2014), that study exhibits higher spatial heterogeneity than we observed at a smaller scale. Similarly, Schaller et al. (2014) observed lower spatial variation in Chinook salmon intrinsic growth rates across Snake River and John Day River populations (Table 2 in Schaller et al. 2014) than Nelson et al. (2019) observed at a smaller spatial scale in Washington state and British Columbia (Table 3 in Nelson et al. 2019).

We predict that increasing SARs from their current level of 0.74% to 1.8% would result in positive population growth in all 23 MFSR segments, indicating that recovery is achievable for genetically and phenotypically diverse stocks in high-quality natal habitats, even at SAR levels near the lower bound of NPCC targets (2%–6%, NPCC 2003). However, Chinook salmon productivity elsewhere in the Snake River ESU may be lower than we observed in the MFSR, resulting in

Fig. 5. Response surface of population growth rate (λ) versus smolt production rate (b) and smolt-to-adult return rate (ϕ_{SAR}). Color indicates population growth rate from red (low) to white (replacement) to blue (high), and the black dotted contour line indicates an isocline of no net population growth (λ=1). The SAR from 2% to 6% represents lower and upper management targets for salmon restoration. Median segment-specific smolt production rates are plotted as black points at the geometric mean ϕ_{SAR} of 0.74% from 1994 to 2018. The arrow represents our simulated increase of SAR from 0.74% up to 2.0%, with gray unfilled circles indicating projected λ for each segment at $\phi_{SAR} = 2.0\%$.

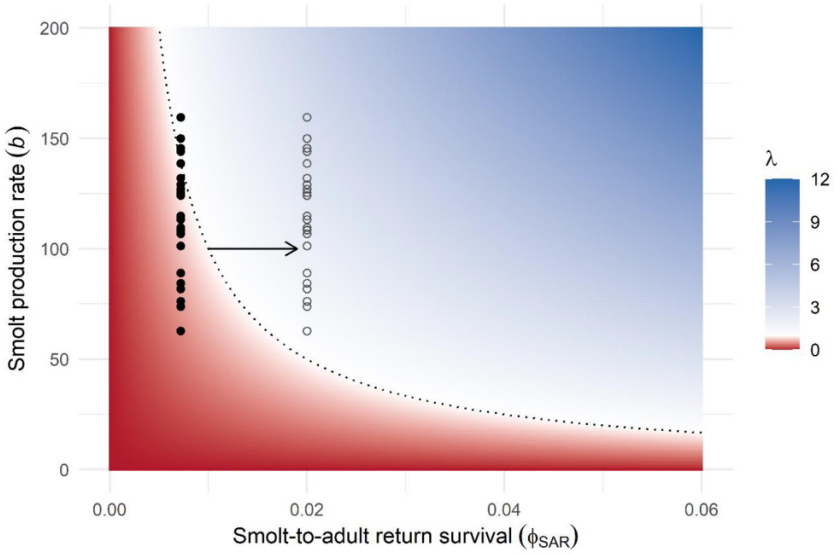

more muted responses to increases in SAR. For example, Idaho's Lemhi and Pahsimeroi Rivers have degraded habitats and narrower salmon genetic diversity compared to the MFSR (IDFG 2019), which may require SARs exceeding 1.8% to realize the population growth benefits we predict for the MFSR. Increasing SARs to meet NPCC goals (2%–6% with a mean of 4%, NPCC 2003) would thus facilitate the rebuilding of less productive Snake River populations, heighten life history diversity and resilience, increase delivery of ocean-derived nutrients and food web subsidies, and rebuild harvestable and sustainable populations (Petrosky et al. 2020; Storch et al. 2022).

Our estimates of Chinook salmon smolt production rates in the MFSR are commensurate with independent estimates for the MFSR and other Snake River spring/summer ESU subpopulations. Our model predicts an average smolt production rate of 104.48 smolts per spawner ($\log.b = 4.489$) and 135 smolts per spawner (90% HDI 95.1–177.2) in the most productive segment (segment "d", comprising most of Marsh Creek). Petrosky et al. (2001) reported that the productivity of Snake River wild Chinook salmon from 1962 to 1997 averaged 86 smolts per spawner. Other estimates of Snake River Chinook salmon productivity are similar. Wilson (2003) estimated that smolt production rates in Marsh Creek (our segment "d") were between 81.4 smolts per spawner (age-3 spawners) and 128.7 smolts per spawner (age 5 spawners) for brood years 1962–1967 and between 61.8 and 97.8 smolts per spawner (respectively) for broodyears 1990–1994. The model of Zabel et al. (2006) suggested that at low spawner density, the productivity of wild Snake River Chinook salmon was 165.1 smolts per spawner, a rate derived from a Beverton-Holt function.

Our results suggest that increasing out-of-basin survival would substantially increase population growth rates of Chinook salmon in the MFSR basin, which corroborates the findings of Marmorek et al. (1998) and McCann et al. (2017, 2019). Under contemporary conditions, the very high mortality of salmon during migratory and marine life stages limits the productivity of Chinook salmon in the MFSR (Schaller et al. 2014; Thurow et al. 2020). Much of that mortality can be explained by the deleterious influence of Columbia and Snake River dams (Raymond 1988; Schaller et al. 1999). Under contemporary conditions, Schaller et al. (2014) estimated that Snake River Chinook salmon smolts, which pass eight dams, survived to adulthood only 1/4 as well as John Day River populations, which pass three dams (Table 5 in Schaller et al. 2014).

Ocean conditions also strongly affect adult salmon returns (Schaller et al. 2014), and climate change is degrading ocean conditions, leading to reduced survival and growth of salmon during marine life stages (Ohlberger et al. 2018; Crozier et al. 2019, 2020, 2021). However, ocean conditions are beyond the immediate control of resource managers, as is climate change (ISAB 2018). In sharp contrast, hydrosystem passage conditions are well within the capabilities of managers to manipulate (ISAB 2018). If SARs continue trending downward because of degraded ocean conditions (Chasco et al. 2017*b*; Crozier et al. 2019), improving conditions in the migration corridor will be of even greater importance (NPCC 2003; Johnson et al. 2021).

Numerous actions have been implemented over the past 40 years to promote the recovery of Snake River Chinook salmon: structural modifications to dams; collection and transportation of juveniles to the LCRE; rehabilitation and enhancement of natal and estuarine habitats; hatchery supple-

mentation; harvest restrictions; reduced landscape development; intensive predator control; reservoir drawdowns; and increased spillover dams (NPCC 2014; Rieman et al. 2015; NMFS 2017). Despite this unprecedented effort, Snake River Chinook salmon still face extinction or extirpation, suggesting that novel, aggressive actions are necessary for recovery (NOAA 2022; Storch et al. 2022). The primary remaining management action to increase SARs is to reduce mortality through the migration corridor and in the ocean by breaching dams (NOAA 2022; AFS 2023). Breaching the four lower Snake River dams and improving spill management for salmon smolts at the remaining four lower Columbia River dams is predicted to increase in-river survival of Snake River Chinook salmon by nearly 22% (Table 2.7 in McCann et al. 2019). Through these direct survival benefits alone, our estimated SAR would increase from 0.74% to 0.90%. However, river restoration is predicted to alleviate both direct and indirect mortality in the migration corridor, estuary, and marine environments (Budy et al. 2002; McCann et al. 2019). In our model, in-river smolt survival was strongly negatively correlated with powerhouse passages ($\beta_{H(3)}$, Table S3), and early ocean survival of the in-river passage group was strongly negatively correlated with water transit time ($\beta_{O(6)}$, Table S3). These results are consistent with evidence that reducing water transit time and powerhouse passages will increase both ocean survival and hydrosystem survival for in-river migrants (Budy et al. 2002; McCann et al. 2019). McCann et al. (2019) predicted that dam breaching would increase ocean survival by 86% and would combine with hydrosystem survival benefits to increase SARs by 2.6-fold (Table 2.10, McCann et al. 2019). A 2.6-fold increase in SARs from our estimated geometric mean of 0.74% would result in a 1.9% SAR, sufficient for all MFSR segments to support positive Chinook salmon population growth (Figs. 4 and 5). Restoration strategies that include breaching all four lower Snake River Dams thus offer the highest probability of elevating MFSR Chinook salmon SARs above 2% (McCann et al. 2020; Storch et al. 2022). Dam removal may also bolster salmon resilience by promoting the expression of more diverse life histories, as Munsch et al. (2023) observed in the Elwha River.

Our model does not structurally estimate the effects of density-dependence. We took this approach because population densities of salmon in the MFSR throughout our study period were at historic lows. For example, spawner abundances in the MFSR from 2017 to 2021 averaged 1.4% of their abundances during the mid-1960s (Thurow et al. 2020; Poole et al. 2022). However, fish that aggregate may still experience density-dependent intraspecific competition at low regional densities if aggregation causes them to experience high local densities (see Lloyd 1967). Indeed, some Columbia/Snake River Chinook salmon populations have exhibited density dependence in somatic growth and survival at low regional densities (Walters et al. 2013; Thorson et al. 2014). If salmon aggregate at low densities but occupy more stream reaches as regional abundances increase (Jacobs et al. 2021), then fish may not actually experience increased crowding, and the intensity of competition might vary little as abundances increase. In this case, our estimates of per-capita smolt production already incorporate effects of density-dependence resulting from localized aggregation (Isaak et al. 2007), and thus our assessment of restoration efforts should be robust to increases in regional adult density. Conversely, if increased regional density of adults depresses per-capita smolt production (e.g., Petrosky et al. 2001; Zabel et al. 2006), then our assessment of restoration efforts may be optimistic and restoration might be more challenging than we have estimated.

We assumed that the MFSR Chinook salmon population segments defined by Isaak and Thurow (2006) represent isolated sub-populations. Although Chinook salmon stray from their natal streams, straying in the MFSR is reported at spatial scales similar to our approximately 30 km segments (Isaak and Thurow 2006; Neville et al. 2006), which is smaller than the straying distances reported for other systems like the upper Columbia River (Hamann and Kennedy 2012). Fortunately, our inferences are unaffected by analyzing data at a larger spatial scale, although larger-scale analyses are less able to evaluate spatial heterogeneity. For example, when we estimated smolt production per spawner at the ICTRT scale, we found slightly higher smolt production per spawner but reduced variance among the 8 sub-populations relative to the current analysis at the ~30 km segment scale with 23 sub-populations (Jacobs 2021). Nevertheless, our results do suggest the influence of some demographic connectivity among segments within the MFSR. The areas with the largest and most contiguous natal habitat patches (Bear Valley and Big Creeks) tended to support the most salmon (Thurow et al. 2020; Jacobs et al. 2021), though these segments were not necessarily the most productive. For example, segments “a”, “b”, and “c” in Bear Valley Creek had the largest redd counts yet supported growth rates roughly equivalent to replacement ($\lambda \approx 1$), with median λ slightly below 1 in each segment. Conversely, neighboring segments (Marsh Creek, Pistol Creek, Upper Mainstem MFSR, and one segment within Big Creek (“w”) had population growth rates above replacement despite relatively small redd counts in those segments (Fig. 1). Therefore, immigration from neighboring segments might be responsible for sustaining the high density in Bear Valley Creek while reducing densities at the neighboring sites. Some dispersal is also required to colonize new habitat patches, such as those caused by debris flows that recruit wood and sediment into streams (Thurow 2015). The extent to which dispersal leads to the colonization of new patches or re-populates stream reaches with few adult salmon warrants further investigation.

Chinook salmon spawner age has declined through time in the MFSR, as the probability of spawning at age 4 (versus 5 or 6) generally increased between 1995 and 2018 from ~25% to ~75% (Fig. S6). This observation is consistent with that of Ohlberger et al. (2018), who found that the age and size of both hatchery and wild Chinook salmon have declined across the Pacific coast. Reductions in the body size of salmon may reduce fecundity, and thus productivity (Healey and Heard 1984). Alternatively, shifts to earlier maturation might increase spawner abundance by reducing the duration of ocean residency and thus ocean mortality (e.g., Cline et al. 2019). We did not account for the effects of reductions in adult size in our model, though we did account for changes in age struc-

ture. A reduction in the diversity of ages at maturation among spawning fish also reduces life history diversity, which may reduce population stability (Schindler et al. 2010). The potential conservation implications of a decline in spawning Chinook salmon age and size in the MFSR thus warrant further investigation.

We conclude that increasing out-of-basin survival will substantially increase population growth rates of Chinook salmon in the MFSR basin. We have refined estimates of SARs needed for population recovery in the MFSR and predict that improving Chinook salmon SARs above 1.8% will lead to positive growth rates across all its sub-populations, though a higher level of SAR may be necessary to support recovery (i.e., increases in abundance) across the larger Snake River ESU (e.g., McCann et al. 2017). High-quality natal habitats, such as those that typify the MFSR, remain capable of supporting viable Chinook salmon populations. However, our results also demonstrate that restoring the Snake River migratory corridor to improve SARs is necessary to realize natal habitat production potential. Despite their extraordinarily long migration past eight major hydroelectric dams, wild Chinook salmon still cling to persistence in the MFSR because of their high genetic and phenotypic diversity and access to exceptional natal habitat. Chinook salmon in the MFSR therefore have very high recovery potential if survival outside the basin can be increased. The results of our analysis are timely and applicable for discussions of management actions and cost–benefit analyses addressing Snake River salmon restoration. Our analysis also demonstrates that spatially explicit time-series data in general, and our long-term spatially continuous Chinook salmon redd dataset in particular, are valuable in ecological research and management contexts.

Acknowledgements

Redd surveys were completed and compiled by R. Thurow with the assistance of skilled helicopter pilots Will Hogan, James Pope Sr., Ron Gipe, and John Hubof. US Forest Service helicopter managers assisted and National Forest dispatch personnel monitored flights. Biologists from IDFG have participated in aerial surveys since 2011. Colleagues from RMRS, IDFG, the Shoshone-Bannock and Nez Perce tribes, and the Payette, Boise, and Salmon-Challis National Forests completed ground-based surveys. Micah Davison (IDFG) provided carcass age data. Steve Haeseker (US Fish and Wildlife Service), Brandon Chockley (Fish Passage Center), and Jerry McCann (Fish Passage Center) provided up-to-date ocean and hydrosystem passage covariates as well as PIT passage counts from the Comparative Survival Study (McCann et al. 2020, 2021). Aerial surveys were funded by RMRS, the Payette National Forest, and the Bonneville Power Administration. John Guzevich, Dave Nagel, and Sharon Payne (RMRS) provided GIS support and review. Suzy Stephens (RMRS) created Fig. 2. Our manuscript was improved from helpful reviews by Steve Haeseker and three anonymous reviewers. Reference to trade names does not imply endorsement by the U.S. Government.

Article information

History dates

Received: 10 June 2023
Accepted: 27 November 2023
Accepted manuscript online: 5 December 2023
Version of record online: 6 February 2024

Copyright

Data availability

Data and products from the Comparative Survival Study (McCann et al. 2019, 2020, 2021) can be obtained from Fish Passage Center reports at https://www.fpc.org/documents/Q_fpc_cssreports.php or by contacting Jerry McCann at jmccann@fpc.org. Data on salmon carcass ages can be obtained with permission from the Idaho Fish and Wildlife Information System (IFWIS) web reports [https://fishandgame.idaho.gov/ifwis/portal]. Data from spatially continuous redd counts in the Middle Fork Salmon River can be obtained from RFT upon reasonable request at russ.thurow@usda.gov. Novel code and data from our analysis are available at https://doi.org/10.5281/zenodo.10117183.

Author information

Author ORCIDs

Gregory R. Jacobs https://orcid.org/0000-0002-3659-1581
Russell F. Thurow https://orcid.org/0000-0002-1362-8599
Charles E. Petrosky https://orcid.org/0000-0001-6059-2288
Craig W. Osenberg https://orcid.org/0000-0003-1918-7904
Seth J. Wenger https://orcid.org/0000-0001-7858-960X

Author contributions

Conceptualization: GRJ, RFT, CEP
Data curation: GRJ, RFT
Formal analysis: GRJ
Investigation: RFT
Methodology: GRJ, RFT
Supervision: CWO, SJW
Validation: CEP
Visualization: GRJ, RFT
Writing – original draft: GRJ
Writing – review & editing: GRJ, RFT, CEP, CWO, SJW

Competing interests

The authors declare there are no competing interests.

Funding information

The authors declare no specific funding for this work.

Supplementary material

Supplementary data are available with the article at https://doi.org/10.1139/cjfas-2023-0167.

References

AFS. 2023. Statement of the American Fisheries Society (AFS) and the Western Division AFS (WDAFS) about the need to breach the four dams on the Lower Snake River. Available from https://fisheries.org/policy-media/recent-policy-statements/statement-of-the-american-fisheries-society-afs-and-the-western-division-afs-wdafs-about-the-need-to-breach-the-four-dams-on-the-lower-snake-river/ [accessed 22 September 2023].

Budy, P., and Schaller, H. 2007. Evaluating tributary restoration potential for Pacific salmon recovery. Ecol. Appl. **17**(4): 1068–1086. doi:10.1890/06-0022. PMID: 17555219.

Budy, P., Thiede, G.P., Bouwes, N., Petrosky, C.E., and Schaller, H.A. 2002. Evidence linking delayed mortality of Snake River salmon to their earlier hydrosystem experience. N. Am. J. Fish. Manage. **22**(1): 35–51. doi:10.1577/1548-8675(2002)022%3c0035:ELDMOS%3e2.0.CO;2.

Chasco, B., Kaplan, I.C., Thomas, A., Acevedo-Gutiérrez, A., Noren, D., Ford, M.J., et al. 2017a. Estimates of Chinook salmon consumption in Washington State inland waters by four marine mammal predators from 1970 to 2015. Can. J. Fish. Aquat. Sci. **74**(8): 1173–1194. doi:10.1139/cjfas-2016-0203.

Chasco, B.E., Kaplan, I.C., Thomas, A.C., Acevedo-Gutiérrez, A., Noren, D.P., Ford, M.J., et al. 2017b. Competing tradeoffs between increasing marine mammal predation and fisheries harvest of Chinook salmon. Sci. Rep. **7**(1): 1–14. doi:10.1038/s41598-017-14984-8. PMID: 28127051.

Cline, T.J., Ohlberger, J., and Schindler, D.E. 2019. Effects of warming climate and competition in the ocean for life-histories of Pacific salmon. Nat. Ecol. Evol. **3**(6): 935–942. doi:10.1038/s41559-019-0901-7. PMID: 31133724.

Conn, P.B., Johnson, D.S., Williams, P.J., Melin, S.R., and Hooten, M.B. 2018. A guide to Bayesian model checking for ecologists. Ecol. Monogr. **88**(4): 526–542. doi:10.1002/ecm.1314.

Copeland, T., and Venditti, D.A. 2009. Contribution of three life history types to smolt production in a Chinook salmon (*Oncorhynchus tshawytscha*) population. Can. J. Fish. Aquat. Sci. **66**(10): 1658–1665. doi:10.1139/F09-110.

Copeland, T., Blythe, D., Schoby, W., Felts, E., and Murphy, P. 2021. Population effect of a large-scale stream restoration effort on Chinook salmon in the Pahsimeroi River, Idaho. River Res. Appl. **37**(1): 100–110. doi:10.1002/rra.3748.

Copeland, T., Venditti, D.A., and Barnett, B.R. 2014. The importance of juvenile migration tactics to adult recruitment in stream-type Chinook salmon populations. Trans. Am. Fish. Soc. **143**(6): 1460–1475. doi:10.1080/00028487.2014.949011.

Crozier, L.G., Burke, B.J., Chasco, B.E., Widener, D.L., and Zabel, R.W. 2021. Climate change threatens Chinook salmon throughout their life cycle. Commun. Biol., **4**(1): 1–14. doi:10.1038/s42003-021-01734-w. PMID: 33398033.

Crozier, L.G., McClure, M.M., Beechie, T., Bograd, S.J., Boughton, D.A., Carr, M., et al., others. 2019. Climate vulnerability assessment for Pacific salmon and steelhead in the California Current Large Marine Ecosystem. PLoS One, **14**(7): e0217711. Public Library of Science San Francisco, CA USA. doi:10.1371/journal.pone.0217711. PMID: 31339895.

Crozier, L.G., Siegel, J.E., Wiesebron, L.E., Trujillo, E.M., Burke, B.J., Sandford, B.P., and Widener, D.L. 2020. Snake River sockeye and Chinook salmon in a changing climate: implications for upstream migration survival during recent extreme and future climates. PLoS One, **15**(9): e0238886. doi:10.1371/journal.pone.0238886. PMID: 32997674.

Denwood, M.J. 2016. runjags: an R package providing interface utilities, model templates, parallel computing methods and additional distributions for MCMC models in JAGS. J. Statist. Software, **71**: 1–25. doi:10.18637/jss.v071.i09.

Esri. (n.d.). World topographic map. [Basemap], 13 June 2013. Available from https://www.arcgis.com/home/item.html?id=30e5fe3149c34df1ba922e6f5bbf808f [accessed 2 June 2023].

Faulkner, J.R., Bellerud, B.L., Widener, D.L., and Zabel, R.W. 2019. Associations among fish length, dam passage history, and survival to adulthood in two at-risk species of Pacific salmon. Trans. Am. Fish. Soc. **148**(6): 1069–1087. doi:10.1002/tafs.10200.

Fausch, K.D., Torgersen, C.E., Baxter, C.V., and Li, H.W. 2002. Landscapes to riverscapes: bridging the gap between research and conservation of stream fishes: a continuous view of the river is needed to understand how processes interacting among scales set the context for stream fishes and their habitat. BioScience, **52**(6): 483–498. doi:10.1641/0006-3568(2002)052%5b0483:LTRBTG%5d2.0.CO;2.

Ford, M.J. 2022. Biological viability assessment update for Pacific salmon and steelhead listed under the Endangered Species Act: Pacific Northwest.

Gelman, A. 2013. Two simple examples for understanding posterior p-values whose distributions are far from uniform. Electron. J. Statist. **7** 2595–2602. doi:10.1214/13-EJS854.

Gelman, A., and Rubin, D.B. 1992. Inference from iterative simulation using multiple sequences. Statist. Sci. **7**(4): 457–472. doi:10.1214/ss/1177011136.

Haeseker, S.L., McCann, J.A., Tuomikoski, J., and Chockley, B. 2012. Assessing freshwater and marine environmental influences on life-stage-specific survival rates of Snake River spring–summer Chinook salmon and steelhead. Trans. Am. Fish. Soc. **141**(1): 121–138. doi:10.1080/00028487.2011.652009.

Hamann, E.J., and Kennedy, B.P. 2012. Juvenile dispersal affects straying behaviors of adults in a migratory population. Ecology, **93**(4): 733–740. doi:10.1890/11-1009.1. PMID: 22690624.

Healey, M.C. and Heard, W.R. 1984. Inter- and Intra-Population Variation in the Fecundity of Chinook Salmon (*Oncorhynchus tshawytscha*) and its Relevance to Life History Theory. Can. J. Fish. Aquat. Sci. **41**(3):476–483. doi:10.1139/f84-057.

Healey, M. 1991. Life history of chinook salmon (*Oncorhynchus tshawytscha*). Pacific salmon life histories. University of British Columbia Press.

Heino, M., Kaitala, V., Ranta, E., and Lindström, J. 1997. Synchronous dynamics and rates of extinction in spatially structured populations. Proc. R. Soc. Lond. B: Biol. Sci. **264**(1381): 481–486. doi:10.1098/rspb.1997.0069.

ICTRT. 2003. Independent populations of Chinook, steelhead, and sockeye for listed evolutionarily significant units within the interior Columbia River domain. Working Draft. Interior Columbia Technical Recovery Team, National Marine Fisheries Service, Northwest Fisheries Science Center, Seattle, WA.

IDFG. 2019. 2019–2024 Fisheries management plan. Idaho Department of Fish and Game. Available from https://idfg.idaho.gov/fish/plans.

Isaak, D.J., and Thurow, R.F. 2006. Network-scale spatial and temporal variation in Chinook salmon (*Oncorhynchus tshawytscha*) redd distributions: patterns inferred from spatially continuous replicate surveys. Can. J. Fish. Aquat. Sci. **63**(2): 285–296. doi:10.1139/f05-214.

Isaak, D.J., Thurow, R.F., Rieman, B.E., and Dunham, J.B. 2003. Temporal variation in synchrony among chinook salmon (*Oncorhynchus tshawytscha*) redd counts from a wilderness area in central Idaho. Can. J. Fish. Aquat. Sci. **60**(7): 840–848. doi:10.1139/f03-073.

Isaak, D.J., Thurow, R.F., Rieman, B.E., and Dunham, J.B. 2007. Chinook salmon use of spawning patches: relative roles of habitat quality, size, and connectivity. Ecol. Appl. **17**(2): 352–364. doi:10.1890/05-1949. PMID: 17489244.

ISAB. 2018. Review of the Comparative Survival Study (CSS) Draft 2018 annual report. Independent Scientific Advisory Board.

Jacobs, G.R. 2021. Population-level consequences of environmental variation for migratory fishes. Ph.D. thesis, University of Georgia, Georgia. Available from https://www.proquest.com/docview/2551582591/abstract/970916E5779048D0PQ/1 [accessed 8 September 2023].

Jacobs, G.R., Thurow, R.F., Buffington, J.M., Isaak, D.J., and Wenger, S.J. 2021. Climate, fire regime, geomorphology, and conspecifics influence the spatial distribution of Chinook salmon redds. Trans. Am. Fish. Soc. **150**(1): 8–23. doi:10.1002/tafs.10270.

Johnson, D., Hesse, J., and Kinser, R. 2021. Nez Perce Tribe staff presentation on their analysis of Snake River basin Chinook and Steelhead—quasi-extinction threshold and call to action. Available from https://www.nwcouncil.org/sites/default/files/2021_05_4.pdf.

Kéry, M., and Schaub, M. 2012. Bayesian population analysis using WinBUGS: a hierarchical perspective. Academic Press.

Lloyd, M. 1967. Mean crowding. J. Anim. Ecol. **36**(1): 1–30. doi:10.2307/3012.

Louhi, P., Vehanen, T., Huusko, A., Mäki-Petäys, A., and Muotka, T. 2016. Long-term monitoring reveals the success of salmonid habitat restoration. Can. J. Fish. Aquat. Sci. **73**(12): 1733–1741. doi:10.1139/cjfas-2015-0546.

Marmorek, D., Peters, C., Parnell, I., Anderson, J., Botsford, L., Bouwes, N., et al., 1998. PATH final report for fiscal year 1998. Bonneville Power Administration, Portland, OR. Citeseer. Available from http://www.efw.bpa.gov/Environment/PATH/reports/ISRP1999CD/PATH%20Reports/WOE _Report/.

Matthews, G.M., and Waples, R.S. 1991. Status review for Snake River spring and summer chinook salmon. National Marine Fisheries Service, Northwest Fisheries Center, Coastal Zone and Estuarine Studies Division.

McCann, J., Chockley, B., Cooper, E., Hsu, B., Schaller, H A, Haeseker, S., et al. 2017. Comparative survival study of PIT-tagged spring/summer/fall Chinook, summer steelhead, and sockeye. 2017 Annual Report, BPA Contract 19960200, Fish Passage Center. Available from https://www.fpc.org/documents/CSS/2017-CSS-Report-Fix.pdf.

McCann, J., Chockley, B., Cooper, E., Hsu, B., Scheer, G., Haeseker, S., et al. 2019. Comparative survival study of PIT-tagged spring/summer/fall Chinook, summer steelhead, and sockeye. 2019 Annual Report, BPA Contract 19960200, Fish Passage Center.

McCann, J., Chockley, B., Cooper, E., Scheer, G., Haeseker, S., Lessard, R., et al. 2020. Comparative survival study of PIT-tagged spring/summer/fall Chinook, summer steelhead, and sockeye. 2020 Annual Report, BPA Contract 19960200, Fish Passage Center. Available from https://www.fpc.org/documents/CSS/2020-CSS-Report.pdf.

McCann, J., Chockley, B., Cooper, E., Scheer, G., Haeseker, S., Lessard, R., et al. 2021. Comparative survival study of PIT-tagged spring/summer/fall Chinook, summer steelhead, and sockeye. 2021 Annual report, BPA Contract 19960200, Fish Passage Center.

McMichael, G.A., Skalski, J.R., and Deters, K.A. 2011. Survival of juvenile Chinook salmon during barge transport. N. Am. J. Fish. Manage. **31**(6): 1187–1196. doi:10.1080/02755947.2011.646455.

Munsch, S.H., McHenry, M., Liermann, M.C., Bennett, T.R., McMillan, J., Moses, R., and Pess, G.R. 2023. Dam removal enables diverse juvenile life histories to emerge in threatened salmonids repopulating a heterogeneous landscape. Front. Ecol. Evol. **11**. Available from https://www.frontiersin.org/articles/10.3389/fevo.2023.1188921 [accessed 9 June 2023]. doi:10.3389/fevo.2023.1188921.

Nehlsen, W., Williams, J.E., and Lichatowich, J.A. 1991. Pacific salmon at the crossroads: stocks at risk from California, Oregon, Idaho, and Washington. Fisheries, **16**(2): 4–21. doi:10.1577/1548-8446(1991)016%3c0004:PSATCS%3e2.0.CO;2.

Nelson, B.W., Walters, C.J., Trites, A.W., and McAllister, M.K. 2019. Wild Chinook salmon productivity is negatively related to seal density and not related to hatchery releases in the Pacific Northwest. Can. J. Fish. Aquat. Sci. **76**(3): 447–462. doi:10.1139/cjfas-2017-0481.

Neville, H.M., Isaak, D.J., Dunham, J.B., Thurow, R.F., and Rieman, B.E. 2006. Fine-scale natal homing and localized movement as shaped by sex and spawning habitat in Chinook salmon: insights from spatial autocorrelation analysis of individual genotypes. Mol. Ecol. **15**(14): 4589–4602. doi:10.1111/j.1365-294X.2006.03082.x. PMID: 17107485.

NMFS. 1992. Endangered and threatened species: threatened status for Snake River spring/summer Chinook salmon, threatened status for Snake River fall Chinook salmon. Fed. Regist. **57**(78): 14563–14663.

NMFS. 2000. Biological opinion of the Federal Columbia River power system including the juvenile fish transportation program and the US Bureau of Reclamation's 31 dams including the entire Columbia Basin project. National Marine Fisheries Service, Seattle, WA.

NMFS. 2017. Recovery plan for Snake River Spring/Summer Chinook salmon and Snake River Basin steelhead. NOAA Fisheries, National Marine Fisheries Service, Portland, OR. Available from https://www.fisheries.noaa.gov/resource/document/recovery-plan-snake-river-spring-summer-chinook-salmon-and-snake-river-basin [accessed 27 September 2023].

NOAA. 2022. Rebuilding Interior Columbia basin salmon and steelhead. National Oceanographic and Atmospheric Administration, National Marine Fisheries Service. Available from https://repository.library.noaa.gov/view/noaa/46461 [accessed 22 September 2023].

NPCC. 2003. Mainstem amendments to the Columbia River basin fish and wildlife program. Council Document 2003-11, Northwest Power and Conservation Council. Available from http://www.nwcouncil.org/fw/program/2003-11/.

NPCC. 2014. Columbia River basin fish and wildlife program. Council Document 2014-12, Northwest Power and Conservation Council. Available from https://www.nwcouncil.org/sites/default/files/2014-12_1.pdf.

Ohlberger, J., Ward, E.J., Schindler, D.E., and Lewis, B. 2018. Demographic changes in Chinook salmon across the Northeast Pacific Ocean. Fish Fish. **19**(3): 533–546. doi:10.1111/faf.12272.

Petrosky, C., and Schaller, H. 2010. Influence of river conditions during seaward migration and ocean conditions on survival rates of Snake River Chinook salmon and steelhead. Ecol. Freshw. Fish, **19**(4): 520–536. doi:10.1111/j.1600-0633.2010.00425.x.

Petrosky, C., Schaller, H., and Budy, P. 2001. Productivity and survival rate trends in the freshwater spawning and rearing stage of Snake River chinook salmon (*Oncorhynchus tshawytscha*). Can. J. Fish. Aquat. Sci. **58**(6): 1196–1207. doi:10.1139/f01-067.

Petrosky, C.E., Schaller, H.A., Tinus, E.S., Copeland, T., and Storch, A.J. 2020. Achieving productivity to recover and restore Columbia River stream-type Chinook Salmon relies on increasing smolt-to-adult survival. N. Am. J. Fish. Manage. **40**(3): 789–803. doi:10.1002/nafm.10449.

Plummer, M. 2017. JAGS: a program for analysis of Bayesian graphical models using Gibbs sampling. Version 4.3.0. Available from http://mcmc-jags.sourceforge.net.

Poole, J., Felts, E.A., Barnett, B., Davison, M., Heller, M., Hand, R., and Brown, E. 2022. Idaho adult Chinook Salmon monitoring. Annual report 2021. IDFG 22–05. Idaho Department of Fish and Game.

Quinn, T.P. 2018. The behavior and ecology of Pacific salmon and trout. University of Washington Press.

R Core Team. 2022. R: a language and environment for statistical computing. R Foundation for Statistical Computing, Vienna, Austria. Available from https://www.R-project.org/.

Raymond, H.L. 1988. Effects of hydroelectric development and fisheries enhancement on spring and summer Chinook salmon and steelhead in the Columbia River basin. N. Am. J. Fish. Manage. **8**(1): 1–24. doi:10.1577/1548-8675(1988)008⟨0001:EOHDAF⟩2.3.CO;2.

Ricker, W.E. 1976. Review of the rate of growth and mortality of Pacific salmon in salt water, and Noncatch mortality caused by fishing. J. Fish. Res. Board Can. **33**(7): 1483–1524. doi:10.1139/f76-191.

Rieman, B.E., Smith, C.L., Naiman, R.J., Ruggerone, G.T., Wood, C.C., Huntly, N., et al. 2015. A comprehensive approach for habitat restoration in the Columbia basin. Fisheries, **40**(3): 124–135. doi:10.1080/03632415.2015.1007205.

Schaller, H.A., Petrosky, C.E., and Langness, O.P. 1999. Contrasting patterns of productivity and survival rates for stream-type Chinook salmon (*Oncorhynchustshawytscha*) populations of the Snake and Columbia Rivers. Can. J. Fish. Aquat. Sci. **56**(6): 1031–1045. doi:10.1139/f99-037.

Schaller, H.A., Petrosky, C.E., and Tinus, E.S. 2014. Evaluating river management during seaward migration to recover Columbia River stream-type Chinook salmon considering the variation in marine conditions. Can. J. Fish. Aquat. Sci. **71**(2): 259–271. doi:10.1139/cjfas-2013-0226.

Schindler, D.E., Hilborn, R., Chasco, B., Boatright, C.P., Quinn, T.P., Rogers, L.A., and Webster, M.S. 2010. Population diversity and the portfolio effect in an exploited species. Nature, **465**(7298): 609–612. doi:10.1038/nature09060. PMID: 20520713.

Slutz, R.J., Lubker, S.J., Hiscox, J.D., Woodruff, S.D., Jenne, R.L., Joseph, D.H., et al. 1985. Comprehensive ocean-atmosphere data set: release 1. NOAA and NCDC, Boulder, CO.

Storch, A.J., Schaller, H.A., Petrosky, C.E., ,Vadas, R.L., Jr, Clemens, B.J., Sprague, G., et al. 2022. A review of potential conservation and fisheries benefits of breaching four dams in the Lower Snake River (Washington, USA). Water Biol. Secur. 100030. 10.1016/j.watbs.2022.100030.

Sutcliffe, O.L., Thomas, C.D., Yates, T.J., and Greatorex-Davies, J.N. 1997. Correlated extinctions, colonizations and population fluctuations in a highly connected ringlet butterfly metapopulation. Oecologia, **109**(2): 235–241. doi:10.1007/s004420050078. PMID: 28307174.

Thorson, J.T., Scheuerell, M.D., Buhle, E.R., and Copeland, T. 2014. Spatial variation buffers temporal fluctuations in early juvenile survival for an endangered Pacific salmon. J. Anim. Ecol. **83**(1): 157–167. doi:10.1111/1365-2656.12117. PMID: 23919254.

Thurow, R. 2015. Salmon, landscapes, and functioning ecosystems: a wilderness lesson in mutual dependency. US Department of Agriculture, Forest Service.

Thurow, R.F. 2000. Dynamics of Chinook salmon populations. *In* Wilderness science in a time of change conference: Missoula, Montana, May

23–27, 1999. United States Department of Agriculture, Forest Service, Rocky Mountain Research Station. p. 143.

Thurow, R.F., Copeland, T., and Oldemeyer, B.N. 2020. Wild salmon and the shifting baseline syndrome: application of archival and contemporary redd counts to estimate historical Chinook salmon (*Oncorhynchus tshawytscha*) production potential in the central Idaho wilderness. Can. J. Fish. Aquat. Sci. **77**(4): 651–665. doi:10.1139/cjfas-2019-0111.

Walters, A.W., Copeland, T., and Venditti, D.A. 2013. The density dilemma: limitations on juvenile production in threatened salmon populations. Ecol. Freshw. Fish, **22**(4): 508–519. doi:10.1111/eff.12046.

Widener, D.L., Faulkner, J.R., Smith, S.G., Marsh, T.M., and Zabel, R.W. 2021. Survival estimates for the passage of spring-migrating juvenile salmonids through Snake and Columbia River dams and reservoirs. p. 2020.

Williams, J.E., Montgomery, D.R., Lichatowich, J.A., Stanford, J.A., Chapman, D., Williams, R.N., et al. 2021. Snake River salmon headed for extinction without drastic action: an open letter to the governors of Washington, Oregon, Idaho, and Montana. Available from https://wildsnakeriversalmon.medium.com/snake-river-salmon-headed-for-extinction-without-drastic-action-e9f0d196eddc.

Wilson, P.H. 2003. Using population projection matrices to evaluate recovery strategies for Snake River spring and summer Chinook salmon. Conserv. Biol. **17**(3): 782–794. doi:10.1046/j.1523-1739.2003.01535.x.

Zabel, R.W., Scheuerell, M.D., McClure, M.M., and Williams, J.G. 2006. The interplay between climate variability and density dependence in the population viability of Chinook salmon. Conserv. Biol. **20**(1): 190–200. doi:10.1111/j.1523-1739.2005.00300.x. PMID: 16909672.

Supplemental material

Life-cycle modeling reveals high recovery potential of at-risk wild Chinook salmon via improved migrant survival.

Contents

1. Parameter descriptions

The parameters, data, and indexes for our statistical life-cycle model of Chinook salmon in the MFSR are described in the main text and in the body of this supplemental material file. To ease interpretation of our model, we have included a comprehensive table to define all 33 parameter objects (matrixes, vectors, and scalars), six data sets, and their indexes at the end of this supplemental material file (Table S1).

2. Parameter estimation

1.1. Life-cycle transitions

We allowed smolt production rate, $b_{(i,t)}$, to vary hierarchically according to a MFSR-wide natural logarithm-transformed mean production rate, $log.b$, and random effects of segment ($\alpha_{b1(i)}$), year ($\alpha_{b2(t)}$), and segment × year ($\alpha_{b3(i,t)}$),

$$b_{(i,t)} = \exp\left(log.b + \alpha_{b1(i)} + \alpha_{b2(t)} + \alpha_{b3(i,t)}\right). \quad (S1)$$

We estimated annual variation in the proportion of Chinook salmon smolts transported from Lower Granite Dam to beyond Bonneville Dam, $\delta_{(t)}$, using a mixed-effects beta regression, in which we allowed estimates to vary according to barge schedule ($\mathrm{Z}_{(t)}$),

$$\mathrm{logit}\left(\delta_{(t)}\right) = \beta_{T(1)} + \beta_{T(2)}\mathrm{Z}_{(t)} + \alpha_{T(t)}. \quad (S2)$$

β_{0T} and β_{1T} are logit-scale regression coefficients and $\alpha_{T(t)}$ is the random effect of year. We included an effect of the shift in the barge transport policy, $\beta_{T(2)}\mathrm{Z}_{(t)}$, following recommendations by Williams et al. (2005). We similarly allowed survival of smolts through the hydrosystem to vary annually according to a mixed-effects beta regression in response to WTT ($X_{WTT(t)}$) and PH ($X_{PH(t)}$) covariates with a random year effect ($\alpha_{H(t)}$)

$$\mathrm{logit}\left(\phi_{H(t)}\right) = \beta_{H(1)} + \beta_{H(2)}X_{WTT(t)} + \beta_{H(3)}X_{PH(t)} + \alpha_{H(t)}. \quad (S3)$$

Early ocean survival was estimated separately for transported and in-river fish using mixed effects logistic regression with both ocean and hydrosystem covariate effects and random year effects. We assumed that summer sea surface temperature ($X_{SST(t)}$), upwelling index ($X_{UWI(t)}$),

summer PDO ($X_{PDO(t)}$), water transit time ($X_{WTT(t)}$), and powerhouse passages ($X_{PH(t)}$) covariates along with a random year effect ($\alpha_{H(t)}$) affected survival in the in-river group,

$$\text{logit}(\phi_{O(t)}) = \beta_{O(1)} + \beta_{O(2)}X_{SST(t)} + \beta_{O(3)}X_{UWI(t)} + \beta_{O(4)}X_{PDO(t)} + \beta_{O(5)}X_{WTT(t)} + \beta_{O(6)}X_{PH(t)} + \alpha_{O(t)}. \quad (S4)$$

We considered an identical model structure for the transported group, except we omitted powerhouse passages and water transit time effects, assuming that a negligible fraction of transported fish experience these in-river conditions,

$$\text{logit}(\phi_{T(t)}) = \beta_{T(1)} + \beta_{T(2)}X_{SST(t)} + \beta_{T(3)}X_{UWI(t)} + \beta_{T(4)}X_{PDO(t)} + \alpha_{T(t)}, \quad (S5)$$

During our study period, few age-6 females returned to the MFSR, which suggested the probability of age-4 marine fish returning as adults at age 5 (ρ_4) was high and its inter-annual variation was negligible; we therefore assumed it was invariant and replaced $\rho_{4(t)}$ in equations 3 and 4 with ρ_4. Our age data and a general trend in declining age structure among Northeast Pacific Salmon (Ohlberger et al., 2018) indicate that the probability of return at age 4, $\rho_{3(t)}$, may have shifted over recent decades. We allow $\rho_{3(t)}$ to vary across years as a random walk evaluated on the logit scale, where we estimate $\rho_{3(t)}$ at time $t = 1$, and an annual deviation, $\alpha_{\rho_3(t-1)}$, drawn form a normal distribution with a mean of zero,

$$\text{logit}(\rho_{3(t)}) = \text{logit}(\rho_{3(t-1)}) + \alpha_{\rho_3(t-1).} \quad (S6)$$

We assume adult return migration survival is equivalent between transport groups and temporally invariant for model simplicity, although transported fish have somewhat lower adult migration survival than in-river fish (Crozier et al., 2020; McCann et al., 2020),

$$\text{logit}(\phi_R) = \beta_R. \quad (S7)$$

We estimated smolt-to-adult return probability for each out-migration year cohort in each MFSR segment as a function of estimated passage transport, hydrosystem smolt survival, early ocean survival, and hydrosystem adult survival (as described above), under assumed ocean survival (ϕ_A=0.8; Ricker, 1976) and barge transport survival of smolts (ϕ_B=0.98; McMichael et al., 2011).

1.2. Cormack-Jolly-Seber sub-model

The Cormack-Jolly-Seber (CJS) capture-mark-recapture model estimates apparent survival from recaptures of marked individual through time under imperfect detection (Cormack, 1964; Jolly, 1965; Seber, 1965). Recaptures are recorded during sampling "occasions" which are discrete points in time when the population is sampled. Occasions in our study are defined by passage facility and life stage mirroring a designation commonly used for smolt-to-adult return passage data: Lower Granite Dam as smolts (LGR), Bonneville Dam as smolts (BON), Bonneville dam as adults (BOA), and Lower Granite Dam as adults (LGA). For the purposes of this mark-recapture analysis, we substitute [passage facility x life stage] for time, such that for adults of a given out-migration cohort, passage at BOA or LGA *at any age* occurs during one "occasion".

Within our full model, we fit multinomial formulations of the Cormack-Jolly-Seber capture-mark-recapture model (Kéry and Schaub, 2012) to estimate survival and observation. Our CJS models were applied to wild spring/summer Chinook salmon PIT tagged and released upstream in the Snake River basin and presented as the wild Snake River aggregate spring/summer Chinook salmon group in the Comparative Survival Study (McCann et al., 2020).

We built two CJS models to explain variation in counts from multinomial capture history summary tables called "m-arrays", one for each smolt passage pathway defined in our model: in-river smolt passage (H group) and transported smolt passage (T group). The m-array is a matrix where each row n is a recapture history for all fish released in the n-th occasion (Table S4, Kéry and Schaub, 2011). We built 2 m-arrays representing recapture histories of Chinook salmon cohorts passing Lower Granite and Bonneville dams, first as smolts and then as adults for the H group (m_H) and the T group (m_T). Cohorts, c, refer to the smolt-migration year, and as such c is equivalent to t during the smolt year. The m-arrays, $m_{T(j,k,t)}$ and $m_{H(j,k,t)}$, are indexed by release occasion (j), recapture occasion (k), and migration year (t). Because T group fish were transported past Bonneville Dam and were thus never observed there, their m-arrays include one less recapture occasion (2 occasions: Bonneville Dam as adults and Lower Granite Dam as adults) than the H group of in-river fish (3 occasions: Bonneville Dam as smolts, Bonneville Dam as adults, Lower Granite Dam as adults) (Table S4). Three key assumptions of these models, given our data, are that upstream survival probabilities across age classes are equivalent (Chapter 5; McCann et al., 2022), that survival probabilities across tributaries of the Snake River are equivalent (and thus reflect the MFSR), and that survival probabilities of males and females are equivalent.

1.2.1.1. *Survival and observation probabilities*

To implement our capture-mark-recapture model, we must model imperfect detection leading to passage observation data because recaptures are a product of both survival and observation probabilities. We allowed observation probability to vary by occasion during our study period, with random variation across years,

105
$$logit\left(p_{(k,c)}\right) = \overline{p}_{(k)} + \alpha_{\bar{p}_{(k,c)}},$$
$$\alpha_{\bar{p}_{(k,c)}} \sim N\left(0, \sigma_{p(k)}\right), \quad (S8)$$

106 where k indexes the recapture occasion, c indexes the migration year cohort, $p_{(k,c)}$ is occasion
107 and cohort-specific observation probability, $\overline{p}_{(k)}$ is the average observation probability of each
108 occasion, and $\alpha_{\bar{p}_{(k,c)}}$ is a random effect of cohort for each occasion, drawn from a normal
109 distribution with a mean of 0 and standard deviation of $\sigma_{p(k)}$. Note that observation probability is
110 indexed by migration year cohort because observations across k occasions occurs at multiple
111 years, but CJS analyses are conducted by cohort. This model structure allows different
112 observation probabilities of smolts vs. returning adults at each dam, and for those probabilities to
113 vary by cohort (and thus across time) as a random effect.

114 Estimation of survival and observation probability across passage facilities for each
115 cohort can then be used to define the multinomial probability of recaptures following each
116 release occasion (row) in the m-array, such as in the generalized example of a four-occasion CJS
117 study presented in Table S5. Several parameters control survival in our model, and apply to
118 distinct life stages that are distributed across CJS sampling occasions, and that vary with time
119 and cohort. Thus, we specified matrixes (π) that correspond to cohort-varying probability vectors
120 of survival rates between recapture occasions in m-array CJS analyses of H and T group
121 survivals (see Fig. 2). For each migration year cohort (indexed by c), H group survival vectors
122 were,

$$
\begin{aligned}
\pi_{H(1,c)} = \quad & \phi_{H(c)}, \\
\pi_{H(2,c)} = \quad & \phi_{O(c)}\phi_A\phi_A\left(1-\rho_{3(c+2)}\right)\phi_A(1-\rho_4) + \\
& \phi_{O(c)}\phi_A\phi_A\left(1-\rho_{3(c+2)}\right)\rho_4 + \\
& \phi_{O(c)}\phi_A\rho_{3(c+2)}, \\
\pi_{H(3,c)} = \quad & \phi_R,
\end{aligned}
\tag{S9}
$$

and T group survival vectors were,

$$
\begin{aligned}
\pi_{T(1,c)} = \quad & \phi_B\phi_{T(c)}\phi_A\phi_A\left(1-\rho_{3(c+2)}\right)\phi_A(1-\rho_4) + \\
& \phi_B\phi_{T(c)}\phi_A\phi_A\left(1-\rho_{3(c+2)}\right)\rho_4 + \\
& \phi_B\phi_{T(c)}\phi_A\rho_{3(c+2)}, \\
\pi_{T(2,c)} = \quad & \phi_R.
\end{aligned}
\tag{S10}
$$

1.2.1.2. Multinomial m-array

In our case, the H group analysis is a four-occasion CJS study with the cell probabilities of its m-array defined as a function of $\pi_{H(k,c)}$ and $p_{(k,c)}$ as follows,

$$
P\left(m_{H(c)}\right) =
$$

$$
\begin{bmatrix}
\pi_{H(1,c)}p_{(1,c)} & \pi_{H(1,c)}\left(1-p_{(1,c)}\right)\times \pi_{H(2,c)}p_{(2,c)} & \pi_{H(1,c)}\left(1-p_{(1,c)}\right)\times \pi_{H(2,c)}\left(1-p_{(2,c)}\right)\times \pi_{H(3,c)}p_{(3,c)} & 1-\pi_{H(1,c)}p_{(1,c)} - \pi_{H(1,c)}\left(1-p_{(1,c)}\right)\pi_{H(2,c)}p_{(2,c)} - \pi_{H(1,c)}\left(1-p_{(1,c)}\pi_{H(2,c)}\left(1-p_{(2,c)}\right)\times \pi_{H(3,c)}p_{(3,c)}\right) \\
0 & \pi_{H(2,c)}p_{(2,c)} & \pi_{H(2,c)}\left(1-p_{(2,c)}\right)\times \pi_{H(3,c)}p_{(3,c)} & 1-\pi_{H(2,c)}p_{(2,c)} - \pi_{H(2,c)}\left(1-p_{(2,c)}\right)\times \pi_{H(3,c)}p_{(3,c)} \\
0 & 0 & \pi_{H(3,c)}p_{(3,c)} & 1-\pi_{H(3,c)}p_{(3,c)}
\end{bmatrix},
\tag{S11}
$$

whereas the T group analysis is a three-occasion CJS study with cell probabilities of its m=array defined as a function of the parameters $\pi_{T(k,c)}$ and $p_{T(k,c)}$,

$$P\left(m_{T(c)}\right) = \begin{bmatrix} \pi_{T(1,c)}p_{T(1,c)} & \pi_{T(1,c)}\left(1-p_{T(1,c)}\right)\times \pi_{T(2,c)}p_{T(2,c)} & 1-\pi_{T(1,c)}p_{T(1,c)} - \pi_{T(1,c)}\left(1-p_{T(1,c)}\right)\times \pi_{T(2,c)}p_{T(2,c)} \\ 0 & \pi_{T(2,c)}p_{T(2,c)} & 1-\pi_{T(2,c)}p_{T(2,c)} \end{bmatrix}. \quad (S12)$$

1.3. Smolt-to-adult returns

The probability vectors $\pi_{H(j,c)}$ and $\pi_{T(j,c)}$, defined in equations S9 and S10 respectively, determine SARs for Chinook salmon overall and in each pathway. To express in terms of migration year t, the SAR of H-group salmon ($SAR_{H(t)}$) was a function of $\phi_{H(t)}$, $\phi_{O(t)}$, ϕ_A, $\rho_{3(t+2)}$, ρ_4, and ϕ_R, the SAR of T-group salmon ($SAR_{T(t)}$) was a function of $\phi_{B(t)}$, $\phi_{T(t)}$, ϕ_A, $\rho_{3(t+2)}$, ρ_4, and ϕ_R, and pathway-specific SARs were weighted by transport pathway probability $\delta_{(t)}$ to predict overall SAR (ϕ_{SAR}),

$$\begin{aligned} SAR_{H(c)} &= \prod_{j=1}^{3} \pi_{H(j,c)}, \\ SAR_{T(c)} &= \prod_{j=1}^{2} \pi_{T(j,c)}, \\ \phi_{SAR(c)} &= \left(1-\delta_{(c)}\right)SAR_{H(c)} + \delta_{(c)}SAR_{T(c)}, \end{aligned} \quad (S13)$$

where c indexes the migration year cohort (all fish that migrated in year $t = c$). Note that our indexing of SARs by smolt migration year (t) is equivalent to indexing by migration year cohort (c), but to remain explicit about indexing parameters that integrate survival and maturation processes across multiple years, we emphasize cohort variation by using the c index for SARs in equations S8 through S13 instead of t.

147 *1.4. Likelihoods*

148 We defined six response variables in our integrated model: $y_{redd(i,t)}$, $y_{age(g_{(i)},t,a)}$,
149 $m_{H(j,k,t)}$, $m_{T(j,k,t)}$, $y_{H(t)}$ and $y_{\delta(t)}$. Subscripts outside of parentheses indicate the data type (e.g.,
150 *redd* representing redd counts). Subscripts inside parentheses index the data matrix (e.g., *i* to
151 index stream segments, *t* to index years). Redd counts, $y_{redd(i,t)}$, vary by segment (i) and year
152 (t). Carcass counts, $y_{age(g_{(i)},t,a)}$, vary spatially by the Interior Columbia Technical Recovery
153 Team (ICTRT, 2003) population that each segment belongs to $(g_{(i)})$, year (t), and age (a).
154 Capture-mark-recapture passage datasets vary by migration year cohort (t) release occasion (j),
155 and passage observation occasion (k), represented by $m_{H(j,k,t)}$ for the in-river smolt passage
156 group and $m_{T(j,k,t)}$ for the transported smolt passage group. Annual point estimates of in-river
157 hydrosystem survival, $y_{H(t)}$, and the proportion of barged fish $(y_{\delta(t)})$ are reported by McCann et
158 al (2020) which provides a more detailed intra-annual smolt survival analysis than we consider
159 here and which derive directly from passage timing data, of which the annual count data we
160 analyze in this manuscript is a simplification.

161 The likelihood of our model is the joint likelihood of our six datasets, conditional on
162 model structure and parameter estimates. First, the likelihoods for $y_{H(t)}$ and $y_{\delta(t)}$ are Beta
163 distribution draws from the probabilities $\phi_{H(t)}$ and $\delta_{(t)}$ (equations S2 and S3, respectively) and
164 the scale coefficients and r_H and r_T, which control variance,

165
$$\begin{aligned} y_{\delta(t)} &\sim \text{Beta}\left(r_\delta\ \delta_{(t)},\ r_\delta\left(1-\delta_{(t)}\right)\right), \\ y_{H(t)} &\sim \text{Beta}\left(r_H\ \phi_{H(t)},\ r_H\left(1-\phi_{H(t)}\right)\right), \end{aligned} \qquad (S14)$$

The number of Chinook salmon from each cohort observed at passage facilities across time is controlled by stage and location-specific survival, maturation, and observation probabilities. To evaluate our CJS models, we used demographic variables to specify probability vectors ($P(m_{H(i,,t)})$ and $P\left(m_{T(i,,t)}\right)$) that define the expected distribution of PIT-tagged fish counts in our m-array mark-recapture capture histories. To predict the number of observed fish from each release at subsequent recapture occasions, we defined the number of fish of each cohort released during each release occasion as $\sum_{k=1}^{4}\left(m_{H(j,k,t)}\right)$ for the H group and $\sum_{k=1}^{3}\left(m_{T(j,k,t)}\right)$ for the T group. We use these quantities to specify the multinomial likelihood of our m-arrays on a per-release-occasion (i.e., m-array row) basis for H group fish,

$$m_{H(j,,t)} \sim \text{Multinomial}\left(P\left(m_{H(j,,t)}\right), \sum_{k=1}^{4}\left(m_{H(j,\text{k},t)}\right)\right), \quad (S15)$$

and for T group fish,

$$m_{T(k,,t)} \sim \text{Multinomial}\left(P\left(m_{T(j,,t)}\right), \sum_{k=1}^{3}\left(m_{T(j,\text{k},t)}\right)\right). \quad (S16)$$

The proportion of female Chinook salmon at each age observed in carcass count data is the result of births, survival, and maturation probabilities. We modeled the number of female carcasses observed at each age in each year, out of a known sample of female carcasses, for each ICTRT population ($g_{(i)}$) as a function of the estimated proportion of returning females at age predicted by our model,

$$y_{age(g_{(i)},t,1:3)} \sim \text{Multinomial}\left(\hat{p}_{age(g_{(i)},t,1:3)}, n_{age(g_{(i)},t)}\right), \quad (S17)$$

where $g_{(i)}$ are the ICTRT populations that the segments (i) are assigned to, $n_{age(g_{(i)},t)}$ is the number of female carcass ages observed at each age in each $g_{(i)}$, and $\hat{p}_{age(g_{(i)},t,1:3)}$ is the estimated proportional contribution of each age (age 4, age 5, and age 6: indexed by 1:3) in year t across all segments within population sub-watershed $g_{(i)}$ in year t. This multinomial likelihood statement informs maturation parameter estimation and helps partition mortality among unobserved at-sea life stages and relatively well-observed migratory life stages.

We model the number of redds observed in segment i at time t ($y_{redd(i,t)}$) as a Poisson draw from $\eta_{(i,t)}$,

$$\begin{aligned} y_{redd(i,t)} &\sim \text{Poisson}(\eta_{(i,t)}), \\ \eta_{(i,t)} &= S_{(i,t)} e^{\varepsilon_{(i,t)}}, \\ \varepsilon_{(i,t)} &\sim \text{Normal}(0, \sigma_{Pois}), \end{aligned} \qquad (S18)$$

where $S_{(i,t)}$ is the latent number of spawning females, $\eta_{(i,t)}$ is the expected number of observations, and $\varepsilon_{(i,t)}$ is a natural logarithm-scale normally-distributed random effect with a mean of 0 and a standard deviation of σ_{Pois}. The $\varepsilon_{(i,t)}$ term accounts for overdispersion in the Poisson count process.

1.5. Priors and constraints

We specified our model to estimate dynamics from 1988 to 2018. To explain initial redd counts in the time series, we hindcast the number of adult female salmon, $S_{(i,t)}$ (i.e., number of redds), in each segment i during each unsurveyed year *t* that may have contributed recruits to spawning runs in 1995 or later (i.e., 1988 – 1994). To do so, we predicted unknown segment redd counts from the empirical relationship between the index redd counts of Brown (2002) and our segment redd counts during the years they overlapped.

We extracted counts from index reaches in the MFSR basin between 1988 and 2000 (Brown, 2002) and summed them by year to define the variable $N_{index(t)}$ which represents the annual sum of ground-based index redd counts in the MFSR. We assumed that the ratio of redd counts in each segment to the sum of redds counted across MFSR index reaches ($\frac{y_{redd(i,t)}}{N_{index(t)}}$) varies by segment with random errors. Specifically, we assumed that the natural logarithm of this ratio in each year varied randomly in time around a segment-specific mean ($\rho_{(i)}$). We fit a linear regression model to estimate the natural logarithm of the ratio between $y_{(i,t)}$ and $N_{index(t)}$ by segment during the years 1995 - 2000,

$$\begin{aligned} \rho_{(i,t)} &= \mathrm{X}\beta + \epsilon_{(i,t)}, \\ \epsilon_{(i,t)} &\sim Normal\left(0, \sigma_{\rho}\right), \end{aligned} \tag{S19}$$

where X is a design matrix of segment indicator variables, β is a vector comprised of an intercept term and n-1 segment-specific coefficients, and ϵ is stochastic error. The fitted model was then used to predict mean and standard error of each segment's $\rho_{(i,t)}$ ($\hat{\rho}_{(i)}$ and $\sigma_{\hat{\rho}_{(i)}}$, respectively),

$$\begin{aligned} \hat{\rho}_{(i)} &= \mathrm{E}\left[\rho_{(i,t)}\right], \\ \sigma_{\hat{\rho}_{(i)}} &= StdErr\left[\hat{\rho}_{(i)}\right]. \end{aligned} \tag{S20}$$

We used these predicted means and standard errors served as priors of the $\xi_{(i,t)}$ variable, which was then multiplied by $N_{index(t)}$ from Brown (2002) to hindcast segment-specific abundances in our model,

$$\begin{aligned} ln\left(\xi_{(i,t)}\right) &\sim Normal\left(\hat{\rho}_{(i)}, \sigma_{\hat{\rho}_{(i)}}\right), \\ ln\left(S_{(i,t)}\right) &= ln\left(N_{index(t)}\right) + ln\left(\xi_{(i,t)}\right), \end{aligned} \tag{S21}$$

We provided an informative Gamma prior for $log.b$, with $\alpha = 64$ and $\beta = 14$, to provide a plausible mean and distribution of numeric scale smolt production rates for Chinook salmon in the MFSR basin based on the literature (e.g., Petrosky et al., 2001), while still constraining the parameter to greater-than-zero values. Logit-scale regression coefficients, $\beta_{T(u)}$, $\beta_{C(u)}$, $\beta_{T(u)}$, and β_R, along with the initial logit-scale return probability of age 4 marine phase female Chinook salmon ($\rho_{3(1)}$), were given Gaussian priors with a mean of 0 and a standard deviation of 2, that are weakly informative on the probability scale (Hobbs and Hooten, 2015; Northrup and Gerber, 2018). As a tuning step to aid model convergence, all logit-scale regression coefficients in equation S3, except $\beta_{H(1)}$ (the intercept term), were given a prior standard deviation of 1 with a mean of 0 to reflect relatively modest covariate effects. We provided an informative Gaussian prior for ρ_4 with a mean of 2 and a standard deviation of 2 on the logit scale (a mean of 0.88 on the probability scale), reflecting evidence that few Snake River Chinook salmon currently remain in the ocean after age 5. Random variance terms, $\alpha_{b1(i)}$, $\alpha_{b2(t)}$, $\alpha_{b3(i,t)}$, $\alpha_{\delta(t)}$, $\alpha_{H(t)}$, $\alpha_{O(t)}$ $\alpha_{T(t)}$, $\alpha_{\rho_3(t-1)}$, and $\varepsilon_{(i,t)}$, were drawn from a Gaussian distribution with a mean of 0 and an estimated standard deviation parameter: σ_{b1}, σ_{b2}, σ_{b3}, σ_{δ}, σ_{H}, σ_{O}, σ_{T}, $\sigma_{\rho 3}$, and σ_{Pois}, respectively. These standard deviations, along with the scale coefficients r_{δ} and r_H used in our Beta regression sub-models used to estimate parameters in equation S2 and S3, were given weakly informative half-Cauchy priors with a mean of 0 and a scale of 2.25 (Gelman, 2006).

We assumed that observation probability was generally consistent across time at each of the passage facilities (regardless of transport group) during our study period, but that each

occasion had distinct observation probability. We defined prior distributions for the logit mean observation probability ($\bar{p}_{(k)}$) and random inter-year variation ($\sigma_{\bar{p}(k)}$),

$$\begin{aligned} \bar{p}_{(k)} &\sim \text{Normal}\left(0, \sqrt{2}\right), \\ \sigma_{\bar{p}(k)} &\sim \text{Half-Cauchy}\left(0, \sqrt{2}\right), \\ \alpha_{\bar{p}(k,c)} &\sim \text{Normal}\left(0, \sigma_{\bar{p}(k)}\right). \end{aligned} \quad (S22)$$

These combined to predict observation probability in each time and at east passage facility from 1994 onward when Snake River PIT passage count data were available. For the H group (and recalling that indexing by migration cohort c is equivalent to t during the migration year),

$$\text{logit}\left(p_{(k,c)}\right) = \bar{p}_{(k)} + \alpha_{\bar{p}(k,c)}. \quad (S23)$$

Since observation probability at each passage facility was assumed identical for H and T groups, but the k-th passage facility was offset for the two groups (T group lacks the BON observation group), p for the T group was defined,

$$\begin{aligned} p_{T(1,c)} &= p_{(2,c)}, \\ p_{T(2,c)} &= p_{(3,c)}. \end{aligned} \quad (S24)$$

1.6. Posterior and joint distributions

An expression of our model's posterior distribution and its proportionality to the joint distribution, where symbols are defined in Table S1, bold regular type represents matrices (e.g., $\mathbf{y_{redd}}$), bold italic type represents vectors (e.g., $\boldsymbol{\beta_H}$), italic type represents scalars (e.g., σ_δ), and bracket notation $[a|b]$ represents a conditional probability distribution (where the probability of a is conditional on b):

$$\begin{aligned}
&\left[\begin{matrix}\mathbf{S},\mathbf{R},\mathbf{N},\mathbf{b},\boldsymbol{\delta},\boldsymbol{\phi_H},\boldsymbol{\phi_O},\boldsymbol{\phi_T},\phi_R,\boldsymbol{\rho_3},\rho_4,\boldsymbol{\beta_H},\boldsymbol{\beta_O},\boldsymbol{\beta_\delta},\boldsymbol{\beta_T},\beta_R,\mathbf{p},\overline{\boldsymbol{p}},\boldsymbol{\eta},\boldsymbol{\xi},\\ \boldsymbol{\sigma_p},\sigma_{b1},\sigma_{b2},\sigma_{b3},\sigma_H,r_H,\sigma_O,\sigma_\delta,r_\delta,\sigma_T,\mu_{\rho3},\sigma_{\rho3},\sigma_{Pois}\end{matrix}\middle|\mathbf{y_{redd}},\mathbf{y_{age}},\boldsymbol{y_\delta},\boldsymbol{y_H},\mathbf{m_H},\mathbf{m_T}\right]\\
&\propto \prod_{i=1}^{s}\prod_{t=1}^{Y}\left[y_{redd(i,t)}|\eta_{(i,t)}\right]\left[\eta_{(i,t)}|S_{(i,t)},\sigma_{Pois}\right]\\
&\times \prod_{g(i)=1}^{8}\prod_{t=1}^{Y}\prod_{a=1}^{3}\left[y_{age(g(i),t,a)}|R_{4(i,t)},R_{5(i,t)},R_{6(i,t)}\right]\\
&\times \prod_{t=1}^{Y}\left[y_{\delta(t)}|\delta_{(t)},r_\delta\right]\\
&\times \prod_{t=1}^{Y}\left[y_{H(t)}|\phi_{H(t)},r_H\right]\\
&\times \prod_{j=1}^{J}\prod_{k=1}^{K}\prod_{t=7}^{Y}\left[m_{H(j,k,t)}|\boldsymbol{\phi_H},\boldsymbol{\phi_O},\phi_R,\boldsymbol{\rho_3},\rho_4,p_{(k,t)}\right]\\
&\times \prod_{j=1}^{J}\prod_{k=1}^{K}\prod_{t=7}^{Y}\left[m_{T(j,k,t)}|\boldsymbol{\phi_T},\phi_R,\boldsymbol{\rho_3},\rho_4,p_{(k,t)}\right]\\
&\times \prod_{k=1}^{K}\prod_{t=7}^{Y}\left[p_{(k,t)}|\overline{p}_{(k,t)},\sigma_{p(k)}\right]\\
&\times \prod_{i=1}^{s}\prod_{t=1}^{Y}\left[\mathbf{S},\mathbf{R},\mathbf{N}|\boldsymbol{\xi},\mathbf{b},\boldsymbol{\delta},\boldsymbol{\phi_H},\boldsymbol{\phi_O},\boldsymbol{\phi_T},\phi_R,\boldsymbol{\rho_3},\rho_4\right]\\
&\times \prod_{t=1}^{Y}\left[\delta_{(t)}|\boldsymbol{\beta_\delta},\sigma_\delta\right]\left[\phi_{H(t)}|\boldsymbol{\beta_H},\sigma_{H,}\right]\left[\phi_{O(t)}|\boldsymbol{\beta_O},\sigma_{O,}\right]\left[\rho_{3(t)}|\mu_{\rho3},\sigma_{\rho3}\right]\\
&\times \left[\rho_4|\mu_{\rho4}\right]\times\left[\phi_R|\beta_R\right]\\
&\times \left[\sigma_{b1},\sigma_{b2},\sigma_{b3},\sigma_H,\sigma_O,\sigma_\delta,\sigma_T,\sigma_{\rho3},r_H,r_\delta,\mu_{\rho3},\mu_4,\boldsymbol{\beta_H},\boldsymbol{\beta_O},\boldsymbol{\beta_\delta},\boldsymbol{\beta_T},\beta_R,\overline{\boldsymbol{p}},\boldsymbol{\sigma_p}\ \sigma_{Pois}\right].
\end{aligned}\tag{S25}$$

2. References

Brown, E.M., 2002. 2000 Salmon spawning ground surveys (IDFG 02–33). Idaho Department of Fish and Game.

Cormack, R.M., 1964. Estimates of Survival from the Sighting of Marked Animals. Biometrika 51, 429–438. https://doi.org/10.2307/2334149

Crozier, L.G., Siegel, J.E., Wiesebron, L.E., Trujillo, E.M., Burke, B.J., Sandford, B.P., Widener, D.L., 2020. Snake River sockeye and Chinook salmon in a changing climate: Implications for upstream migration survival during recent extreme and future climates. PloS one 15, e0238886.

Gelman, A., 2006. Prior distributions for variance parameters in hierarchical models (comment on article by Browne and Draper). Bayesian Analysis 1, 515–534. https://doi.org/10.1214/06-BA117A

Hobbs, N.T., Hooten, M.B., 2015. Bayesian Models: A Statistical Primer for Ecologists. Princeton University Press, Princeton. https://doi.org/doi:10.1515/9781400866557

ICTRT, 2003. Independent populations of Chinook, steelhead, and sockeye for listed evolutionarily significant units within the interior Columbia River domain. Working Draft.

Jolly, G.M., 1965. Explicit estimates from capture-recapture data with both death and immigration-stochastic model. Biometrika 52, 225–247.

Kéry, M., Schaub, M., 2012. Bayesian population analysis using WinBUGS: a hierarchical perspective. Academic Press.

McCann, J., Chockley, B., Cooper, E., Scheer, G., Haeseker, S., Lessard, R., Copeland, T., Ebel, J., Storch, A., Rawding, D., 2022. Comparative survival study of PIT-tagged spring/summer/fall Chinook, summer steelhead, and sockeye (2022 Annual Report, BPA Contract 19960200). Fish Passage Center.

McCann, J., Chockley, B., Cooper, E., Scheer, G., Haeseker, S., Lessard, R., Copeland, T., Ebel, J., Storch, A., Rawding, D., 2020. Comparative survival study of PIT-tagged spring/summer/fall Chinook, summer steelhead, and sockeye (2020 Annual Report, BPA Contract 19960200). Fish Passage Center.

McMichael, G.A., Skalski, J.R., Deters, K.A., 2011. Survival of Juvenile Chinook Salmon during Barge Transport. North American Journal of Fisheries Management 31, 1187–1196. https://doi.org/10.1080/02755947.2011.646455

Northrup, J.M., Gerber, B.D., 2018. A comment on priors for Bayesian occupancy models. PLOS ONE 13, 1–13. https://doi.org/10.1371/journal.pone.0192819

Ohlberger, J., Ward, E.J., Schindler, D.E., Lewis, B., 2018. Demographic changes in Chinook salmon across the Northeast Pacific Ocean. Fish and Fisheries 19, 533–546. https://doi.org/10.1111/faf.12272

Petrosky, C., Schaller, H., Budy, P., 2001. Productivity and survival rate trends in the freshwater spawning and rearing stage of Snake River chinook salmon (*Oncorhynchus tshawytscha*). Canadian Journal of Fisheries and Aquatic Sciences 58, 1196–1207.

Ricker, W.E., 1976. Review of the Rate of Growth and Mortality of Pacific Salmon in Salt Water, and Noncatch Mortality Caused by Fishing. Journal of the Fisheries Research Board of Canada 33, 1483–1524. https://doi.org/10.1139/f76-191

Seber, G.A.F., 1965. A note on the multiple-recapture census. Biometrika 52, 249–260. https://doi.org/10.1093/biomet/52.1-2.249

Williams, J.G., Smith, S.G., Zabel, R.W., Muir, W.D., Scheuerell, M.D., Sandford, B.P., Marsh, D.M., McNatt, R.A., Achord, S., 2005. Effects of the federal Columbia River power system on salmonid populations (NOAA Technical Memorandum NMFS-NWFSC-63). US Department of Commerce.

3. Tables

Table S1. Symbols used in the model and their definitions. Bold regular type represents matrices (e.g., $\mathbf{y_{redd}}$), bold italic type represents vectors (e.g., $\boldsymbol{\beta_H}$), and italic type represents scalars (e.g., σ_δ).

Indexes	Definition
i	Stream segment index from 1 through s=23.
$g(i)$	The ICTRT population of each stream segment.
t	Year index from 1 through Y=32.
c	Migration year cohort index from 1 through Y=32 ($c = t$ during the migration year).
a	Age index, used when determining age distribution of spawners where ages 4, 5, and 6 are indexed by a=1 through A=3.
j	CJS release occasion index.
k	CJS recapture occasion index.
Data	
$\mathbf{y_{redd}}$	Redd counts indexed by stream segment and year, $y_{redd(i,t)}$.
$\mathbf{y_{age}}$	Ages of adult carcasses after spawning in the MFSR, indexed by the ICTRT population, year, and age, $y_{age(g(i),t,a)}$.
$\boldsymbol{y_\delta}$	Annual point estimates of the proportion of barged fish, $y_{\delta(t)}$ from McCann et al. (2020).
$\boldsymbol{y_H}$	Annual point estimates of in-river hydrosystem survival, $y_{H(t)}$ from McCann et al. (2020).
$\mathbf{m_H}$	Capture-mark-recapture passage dataset for the in-river smolt passage group, indexed by migration year cohort (t), release occasion (j), and passage observation occasion (k), $m_{H(j,k,t)}$.
$\mathbf{m_T}$	Capture-mark-recapture passage dataset for the transported smolt passage group, indexed by migration year cohort (t), release occasion (j), and passage observation occasion (k), $m_{T(j,k,t)}$.
Parameters	
$\mathbf{S}$	A matrix of counts of spawning adult Chinook salmon indexed by segment and year, $S_{(i,t)}$.
$\mathbf{R}$	A matrix of counts of returning adult Chinook salmon indexed by age (age 4, 5, and 5), segment, and year, $R_{4(i,t)}, R_{5(i,t)}, R_{6(i,t)}$.
$\mathbf{N}$	A matrix of counts of immature Chinook salmon indexed by age (age 1 though 5), segment, and year, $N_{1(i,t)}, N_{2(i,t)}, N_{3(i,t)}, N_{4(i,t)}, N_{5(i,t)}$.
$\mathbf{b}$	A matrix of smolt production rate (number of smolts produced per spawning female) indexed by segment and year, $b_{(i,t)}$.
$\boldsymbol{\delta}$	A vector of the proportion of out-migrating Chinook salmon smolts that experience the "transport" pathway through the Columbia River, indexed by year, $\delta_{(t)}$
$\boldsymbol{\phi_H}$	A vector of hydrosystem survival probabilities – survival during in-river outmigration of Chinook salmon smolts – as a function of hydrosystem conditions during the migration year, indexed by year, $\phi_{H(t)}$.

$\boldsymbol{\phi_O}$ A vector of survival probabilities of "in-river" group Chinook salmon smolts while migrating through the Columbia River estuary and nearshore Pacific Ocean through their first winter at sea, indexed by year, $\phi_{O(t)}$.

$\boldsymbol{\phi_T}$ A vector of survival probabilities for "transport" group Chinook salmon smolts while migrating through the Columbia River estuary and nearshore Pacific Ocean through their first winter at sea, indexed by year, $\phi_{T(t)}$.

ϕ_R Survival probability of returning adult Chinook salmon to account for mortality as adults migrate upstream through the hydrosystem.

$\boldsymbol{\rho_3}$ A vector of maturation probabilities of ocean-resident age-3 Chinook salmon, indexed by year, $\rho_{3(t)}$.

ρ_4 Maturation probability of ocean-resident age-4 Chinook salmon.

$\boldsymbol{\beta_H}$ Vector of regression coefficients explaining variation in hydrosystem survival of "in-river" group smolts

$\boldsymbol{\beta_O}$ Vector of regression coefficients explaining variation in early ocean survival of "in-river" group smolts

$\boldsymbol{\beta_\delta}$ Vector of regression coefficients explaining variation in the probability of transport vs. in-river passage

$\boldsymbol{\beta_T}$ Vector of regression coefficients explaining variation in early ocean survival of "transport" group smolts

β_R The logit transform of the survival probability of returning adult Chinook salmon.

$\mathbf{p}$ A matrix of observation probabilities in the capture-mark-recapture passage analysis, indexed by occasion and migration year corhort, $p_{(k,c)}$ or equivalently expressed by migration year (though recognizing that true years vary across k), $p_{(k,t)}$.

$\overline{\boldsymbol{p}}$ A vector of average expected observation probabilities in the capture-mark-recapture passage analysis, indexed by occasion, $\overline{p}_{(k)}$

$\boldsymbol{\eta}$ A matrix of the expected number of redd observations, indexed by segment and year, $\eta_{(i,t)}$

$\boldsymbol{\xi}$ A matrix of ratios of redd counts in each segment and each year to redd counts in the index survey data presented by Brown (2002) for the time period 1988-2000, indexed by segment and year, $\xi_{(i,t)}$.

$\boldsymbol{\sigma_p}$ A vector of standard deviations of random variation in observation probability in the capture-mark-recatpure dataset, indexed by occasion, $\sigma_{p(k)}$

σ_{b1} The standard deviation of random variation in smolt production rate among segments.

σ_{b2} The standard deviation of random variation in smolt production rate among years.

σ_{b3} The standard deviation of random variation in smolt production rate across years and segments.

σ_H The standard deviation of random variation in in-river smolt passage survival among years.

r_H The scale coefficient for the beta regression predicting in-river group smolt survival.

σ_O	The standard deviation of random variation in early-ocean smolt survival for the in-river passage group among years.
σ_δ	The standard deviation of random variation in transport probability among years.
r_δ	The scale coefficient for the beta regression predicting the proportion of transported smolts.
σ_T	The standard deviation of random variation in early-ocean smolt survival for the transported passage group among years
$\mu_{\rho 3}$	The maturation probability for age-3 ocean resident Chinook salmon among years at the beginning of our study.
$\sigma_{\rho 3}$	The standard deviation of random walk variation in maturation probability for age-3 ocean resident Chinook salmon among years.
σ_{Pois}	The standard deviation of random variation in the expected number of redd observations.

326

Table S2. Number and age distribution of female Chinook salmon carcasses collected in eight ICTRT (2003) populations within the Middle Fork Salmon River (Fig. 1), 1998-2019

MFSR Sub-basin	Population	Age 4	Age 5	Age 6	Total
Lower	Big Creek	157	99	5	261
Lower	Camas Creek	80	50	0	130
Lower	Loon Creek	41	31	0	72
Lower	Lower Management Area	0	0	0	0
Upper	Sulphur Creek	143	57	0	200
Upper	Upper Management Area	4	3	0	7
Upper	Bear Valley Creek	357	464	14	835
Upper	Marsh Creek	408	395	8	811
Total		1190	1099	27	2316

Table S3. Median and 90% highest density interval (lHDI to hHDI) for stochastic model parameters. Indexes for β_δ refer to (1) intercept, (2) barge schedule. Indexes for β_H refer to (1) intercept, (2) water transit time, and (3) number of powerhouse passages. Indexes for β_O refer to (1) intercept, (2) SST, (3) UWI, (4) MJJ PDO, (5) WTT, and (6) PH. Indexes for β_T refer to (1) intercept, (2) SST, (3) UWI, and (4) MJJ PDO. Indexes on $\bar{p}$ and σ_p refer to PIT tag observation occasions of (1) BON, (2) BOA, and (3) LGA.

Parameter	Median	lHDI	hHDI
$\beta_{\delta(1)}$	1.265	0.897	1.639
$\beta_{\delta(2)}$	-1.96	-2.466	-1.441
$\beta_{H(1)}$	0.135	-0.023	0.288
$\beta_{H(2)}$	-0.042	-0.224	0.135
$\beta_{H(3)}$	-0.332	-0.511	-0.145
$\beta_{O(1)}$	-3.911	-4.13	-3.693
$\beta_{O(2)}$	-0.345	-0.572	-0.119
$\beta_{O(3)}$	0.445	0.177	0.734
$\beta_{O(4)}$	-0.146	-0.408	0.118
$\beta_{O(5)}$	-0.408	-0.654	-0.17
$\beta_{O(6)}$	-0.016	-0.352	0.314
β_R	1.933	1.388	2.72
$\beta_{T(1)}$	-4.361	-4.566	-4.159
$\beta_{T(2)}$	-0.118	-0.307	0.065
$\beta_{T(3)}$	0.448	0.158	0.728
$\beta_{T(4)}$	-0.26	-0.496	-0.018
$log.b$	4.649	4.214	5.082
$\bar{p}_1$	-1.935	-2.286	-1.573
$\bar{p}_2$	2.083	1.031	3.117
$\bar{p}_3$	2.262	1.471	3.221
$\mu_{\rho 3}$	-0.178	-1.838	1.475
$\mu_{\rho 4}$	3.41	3.102	3.722
r_δ	11.12	3.725	27.022
r_H	49.244	11.174	139.324
σ_{b1}	0.274	0.183	0.377
σ_{b2}	1.685	1.26	2.154
σ_{b3}	0.322	0.225	0.421
σ_δ	0.367	0	0.707
σ_H	0.375	0.21	0.55
σ_O	0.538	0.37	0.728
$\sigma_{p(1)}$	1.057	0.778	1.373
$\sigma_{p(2)}$	3.43	2.487	4.496
$\sigma_{p(3)}$	0.274	0	0.658
σ_{Pois}	0.306	0.26	0.354
$\sigma_{\rho 3}$	0.894	0.644	1.187
σ_T	0.505	0.342	0.691

Table S4. An example m-array taken from our data on the in-river group for migration year 2018. To interpret the table, the first row indicates the recapture histories for fish tagged during the first occasion, indicating that 557+51+1+8044=8653 fish were tagged during the first occasion, 557 were next observed passing the Lower Granite Dam as smolts, 51 were next observed passing Bonneville Dam as Smolts, 1 was next observed passing Bonneville Dam as an adult, and 8044 fish were never re-observed. The second row indicates that of the 7+0+550=557 fish that were observed during the second occasion, 7 were observed passing Bonneville Dam as smolts, none were observed passing Bonneville Dam as adults, and 550 were never reobserved. The third row indicates that of the 47+11=58 fish that were observed during the second occasion, 47 were observed passing Lower Granite Dam as adults and 11 were never reobserved

	Recapture Occasion			
Release Occasion	2 (BON)	3 (BOA)	4 (LGA)	Never recaptured
1 (LGR)	557	51	1	8044
2 (BON)	0	7	0	550
3 (BOA)	0	0	47	11

Table S5. The expected values of the entries of the m-array for a four occasion Cormack-Jolly-Seber capture-mark-recapture study, based on the underlying model parameters for survival (ϕ) and observation probability (p), and the number of released individuals. Each row's cell probabilities comprise the multinomial distribution for each release occasion. Note that multi-line entries in cells of columns 3 and 4 are products, e.g., cell (1,3) is the product $\phi_1(1-p_1)\phi_2 p_2$.

	Recapture Occasion			
Release Occasion	2	3	4	Never recaptured
1	$\phi_1 p_1$	$\phi_1(1-p_1)$ $\phi_2 p_2$	$\phi_1(1-p_1)$ $\phi_2(1-p_2)$ $\phi_3 p_3$	$1-\phi_1 p_1-\phi_1(1-p_1)\phi_2 p_2$ $-\phi_1(1-p_1\phi_2(1-p_2)\phi_3 p_3$ $=1-\sum$(rel. occ 1)
2	0	$\phi_2 p_2$	$\phi_2(1-p_2)$ $\phi_3 p_3$	$1-\phi_2 p_2-\phi_2(1-p_2)\phi_3 p_3$ $=1-\sum$(rel. occ 2)
3	0	0	$\phi_3 p_3$	$1-\phi_3 p_3=1-\sum$(rel. occ 3)

4. Figures

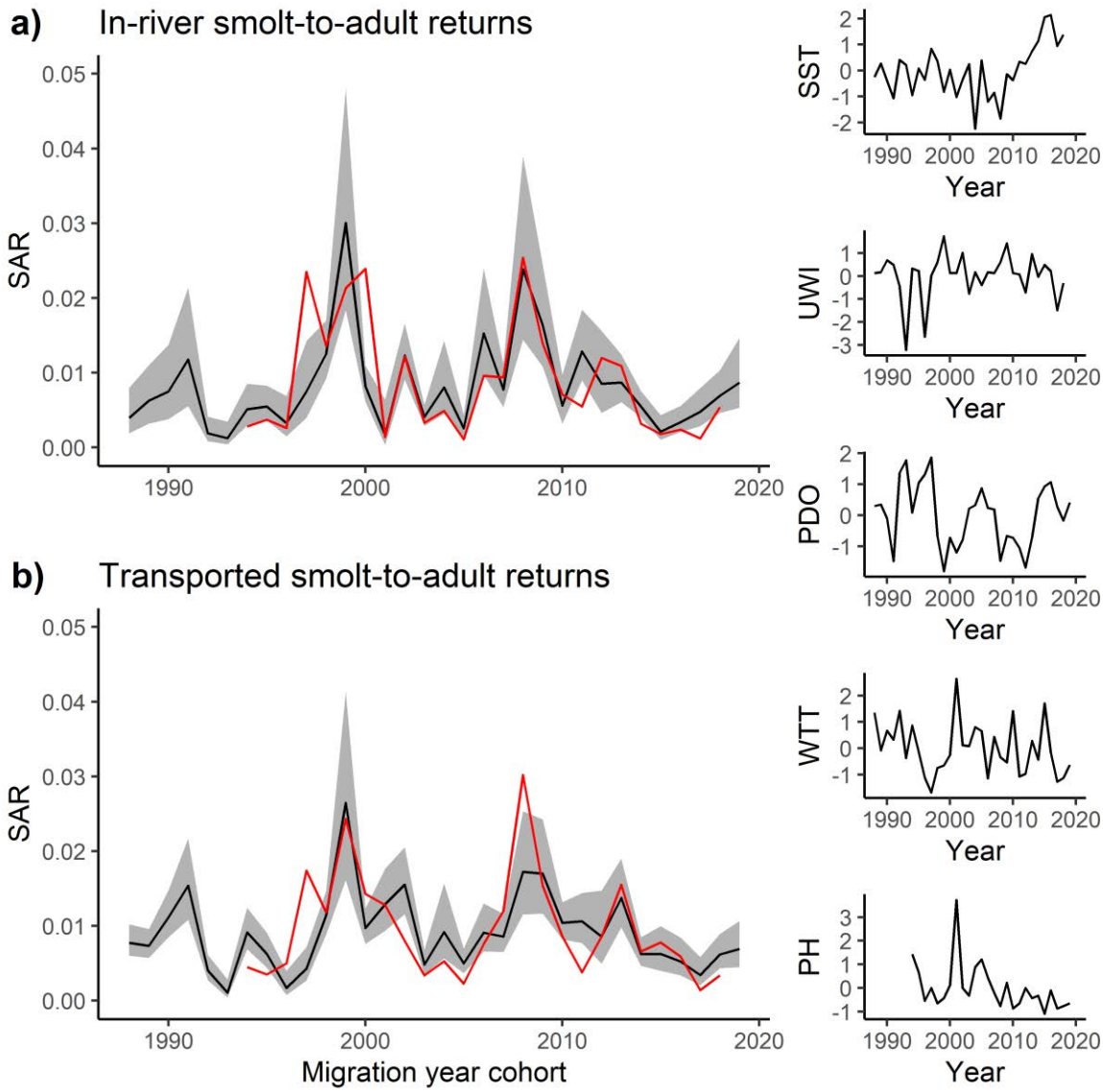

Fig. S1. Posterior median and 90% credible interval of smolt-to-adult survival rate (SARs) across out-migration year for in-river (H group, panel a) and transported (T group, panel b) Chinook salmon smolt passage groups. Posterior estimates are conditional on random among-year variation. The red line traces annual estimates of SARs for the corresponding passage group in the Comparative Survival Study (McCann et al. 2020). Sub-panels on the right margin show annual variation in the covariates we used to explain Chinook salmon survival: Sea surface temperature (SST), April Bakun upwelling index (UWI), Average Pacific Decadal Oscillation index during May, June, and July (PDO), Columbia River hydrosystem water transit time (WTT), and the average number of powerhouse passages by smolts migrating through the Columbia River hydrosystem (PH).

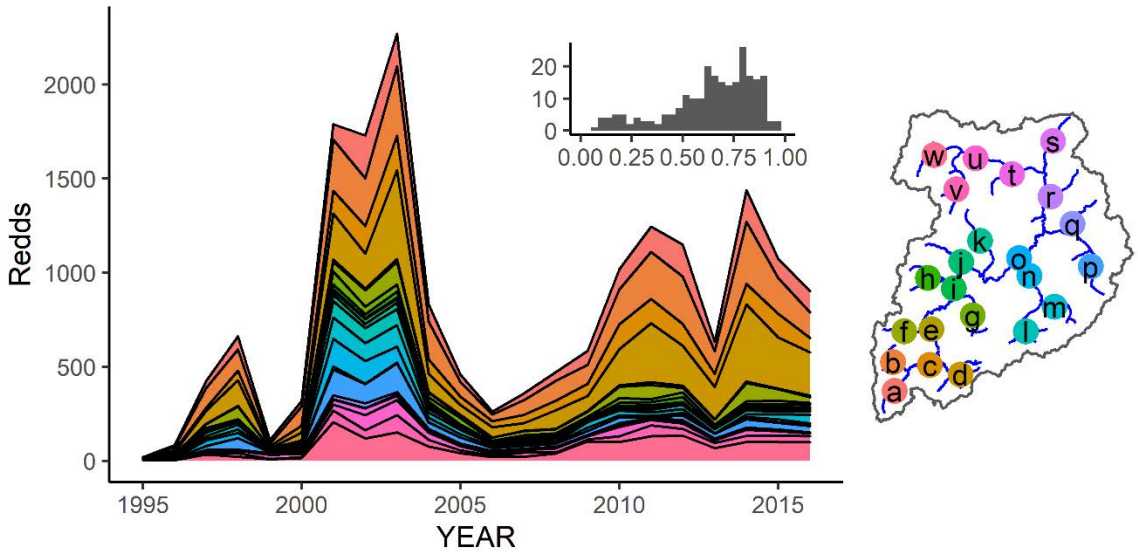

347

348 **Fig. S2.** A stacked time-series plot of annual Middle Fork Salmon River redd counts divided into
349 stream segments denoted by Isaak and Thurow (2006). The sub-panel in the upper right corner of
350 the time-series plot shows the distribution of pairwise Pearson's correlation coefficients among
351 segments. The map key denotes the letter label of each segment, and maps by color to the
352 stacked time-series plot.

353

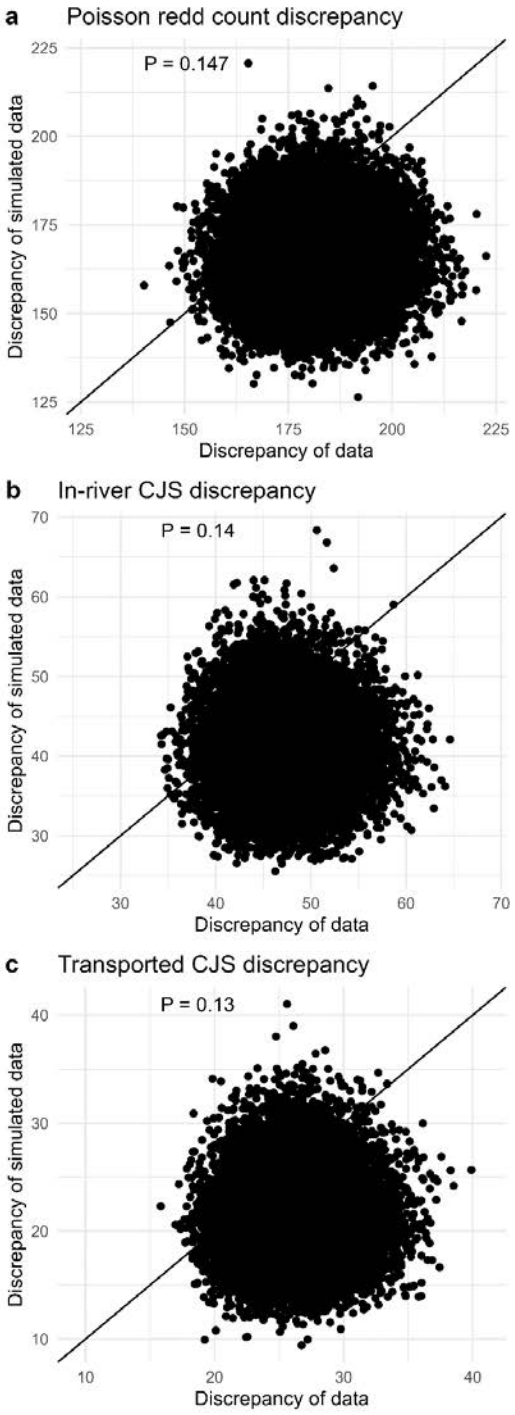

Fig. S3. Posterior predictive checks of Freeman-Tukey discrepancy statistics for redd counts and cohort-specific Cormack-Jolly-Seber (CJS) survival sub-models. Panels a describes the discrepancy associated with the Poisson redd counts, panel b describes the discrepancy associated with the CJS models of fish that out-migrate via the in-river pathway (H group), and panel c describes the discrepancy associated with the CJS model of fish that out-migrate via the transport pathway (T group).

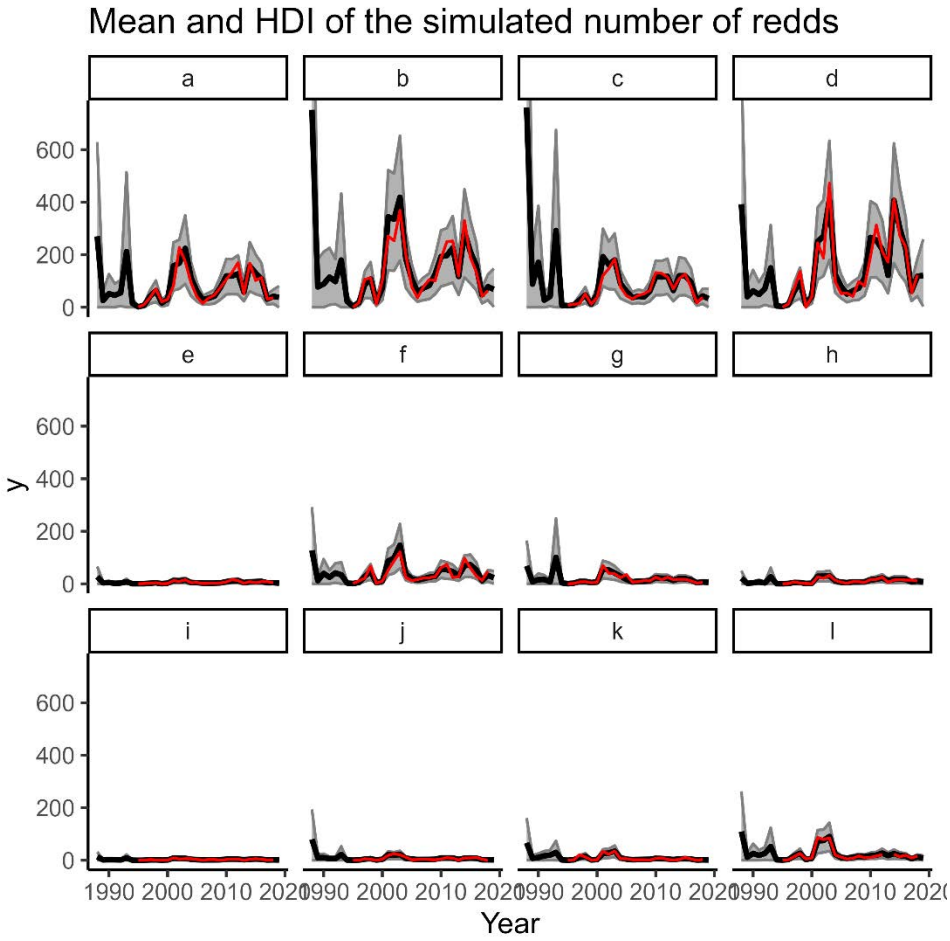

Fig. S4. (Page 1/2) Figure showing the correspondence between observed and simulated redd counts over time in each MFSR stream segment. Gray ribbons are the 90% highest density interval, grey lines are the average simulated redd count at each time point, and black dots are observed redds from our dataset. Panels are labeled by stream segment (Fig 1). Note: this figure includes 23 panels across 2 pages. (1/2)

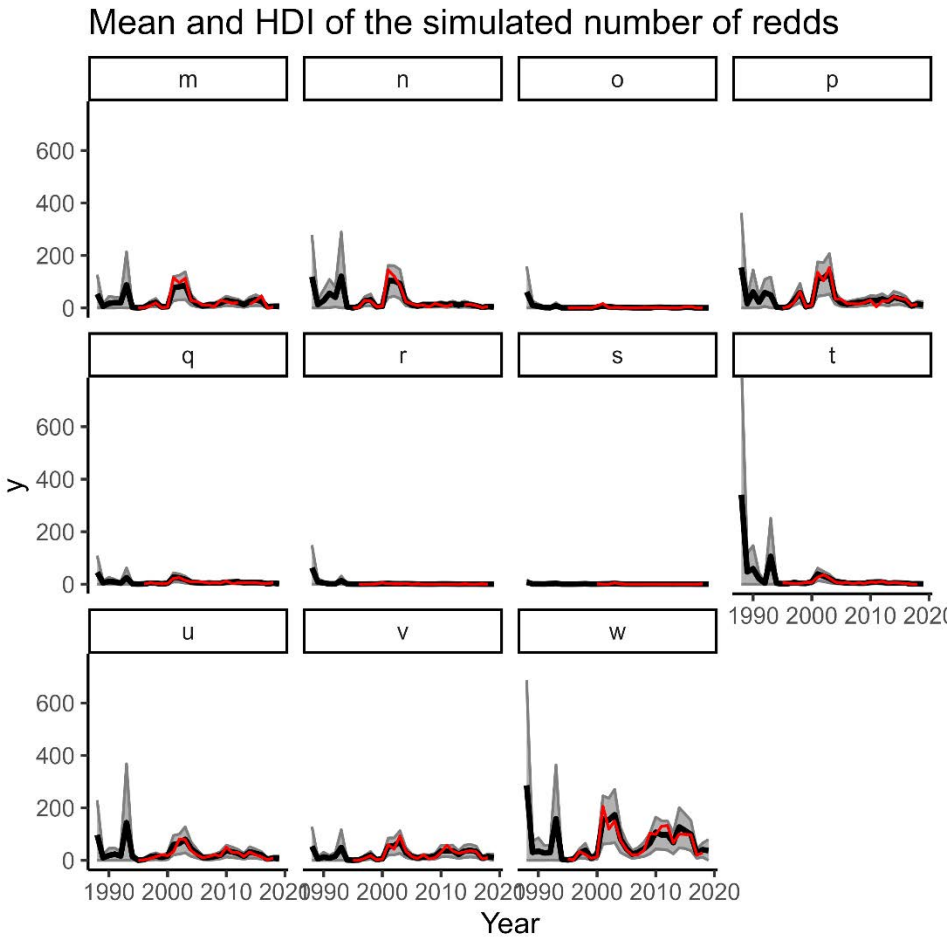

Fig. S4. (Page 2/2) Figure showing the correspondence between observed and simulated redd counts over time in each MFSR stream segment. Gray ribbons are the 90% highest density interval, grey lines are the average simulated redd count at each time point, and black dots are observed redds from our dataset. Panels are labeled by stream segment (Fig 1). Note: this figure includes 23 panels across 2 pages.

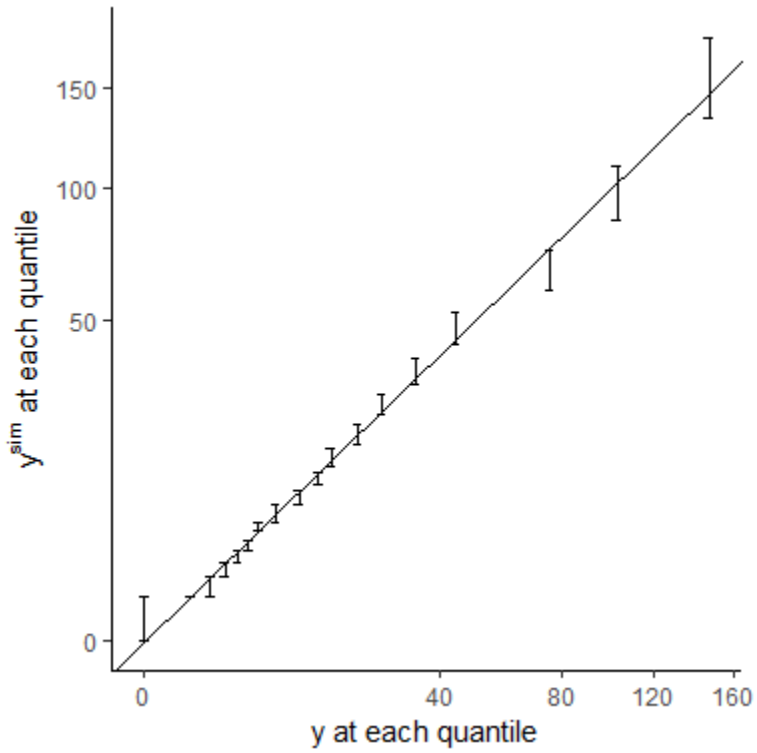

Fig. S5. Visual quantile distribution check for the redd count dataset (y) versus simulated redd counts (y^{sim}). We estimated the 5th through 95th percentiles of redd counts and that of simulated redd counts across segments and time (at 5% intervals) for each posterior sampling iteration in each chain. We then plotted distributions of simulated quantiles against corresponding data quantiles and compared to a 1:1 line to evaluate posterior predictive performance across the data distribution. Whiskers are the 95% credible intervals. Axes are square root-scaled (instead of log-scaled) to facilitate visualization without omitting zeros.

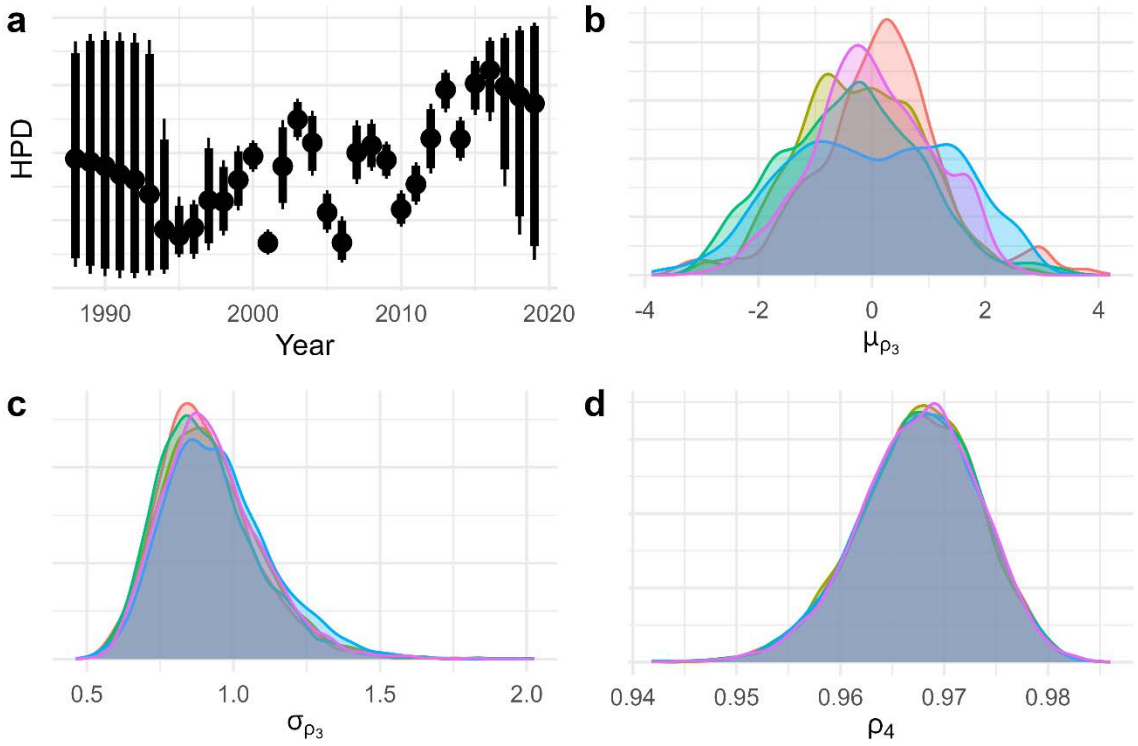

Fig. S6. Age-at-return predictions and parameters. Panel a shows the posterior median probability that age 3 fish return to spawn at age 4 across years with 90% (thick line) and 95% (thin line) credible intervals. Panel b shows the posterior distribution of μ_{ρ_3} on the logit scale, which is equal to the logit transform of the initial maturation probability, $\rho_{3(1)}$. Panel c shows the posterior distribution of σ_{ρ_3} on the logit scale, which controls temporal variation in step size and direction in the random walk equation. Panel d shows the posterior distribution of ρ_4 on the probability scale, representing the probability that age 4 ocean fish will return to spawn at age 5. In our model, all age 5 ocean fish return to spawn at age 6.